PHONON RENORMALIZATION EFFECTS IN LOW DIMENSIONAL ELECTRON-HOLE SYSTEMS

A THESIS
SUBMITTED TO THE DEPARTMENT OF PHYSICS
AND THE INSTITUTE OF ENGINEERING AND SCIENCE
OF BİLKENT UNIVERSITY
IN PARTIAL FULFILLMENT OF THE REQUIREMENTS
FOR THE DEGREE OF
MASTER OF SCIENCE

By
Kaan Güven
September 1995

I certify that I have read this thesis and that in my opinion it is fully adequate, in scope and in quality, as a dissertation for the degree of Master of Science.

Assoc. Prof. Bilal Tanatar (Supervisor)

I certify that I have read this thesis and that in my opinion it is fully adequate, in scope and in quality, as a dissertation for the degree of Master of Science.

Prof. Atilla Erçelebi

I certify that I have read this thesis and that in my opinion it is fully adequate, in scope and in quality, as a dissertation for the degree of Master of Science.

Prof. Atilla Aydınlı

Approved for the Institute of Engineering and Science:

Prof. Mehmet Baray
Director of Institute of Engineering and Science

Abstract

PHONON RENORMALIZATION EFFECTS IN LOW DIMENSIONAL ELECTRON-HOLE SYSTEMS

Kaan Güven
M. S. in Physics
Supervisor: Assoc. Prof. Bilal Tanatar
September 1995

Low dimensional semiconductor structures have been an extensive research area in condensed matter physics. In particular, much effort has been devoted to the study of quasi-one-dimensional semiconductor structures in recent years. The new physical phenomena involved in these systems arising due to the reduced dimensionality point to various potential applications for future technologies. Although the theory is familiar with the "one-dimensional" problem for a long time, the realization of such structures (also known as quantum wires) extends only to a decade before. However, the novel production techniques led to a rapid increase in the experimental studies which, in turn, required a more realistic and comprehensive theory to analyze and interpret the obtained data. This thesis work intends to make a contribution in the direction of these improvements.

Our study is based on a quasi-one-dimensional electron-hole system as realized in photoexcited quantum wires, interacting with the bulk LO-phonons. We investigate the polaronic corrections to the band gap and the carrier effective mass, and the dependence of this correction itself to carrier density, temperature, and quantum finite size effects. We apply two different formal approaches;

the perturbation theory and the variational method. The latter enables the investigation of dynamical screening effects, thereby clarifying the question of validity of the static screening approximation in one dimension. Our results have shown that dynamical screening is relevant in low dimensions. The dielectric function, which is a key quantity in describing the many-particle properties, is analyzed under different approximations such as the Hartree-Fock approximation, random-phase approximation, and the more advanced local-field correction. Several confinement potentials (infinite well, parabolic, cylindrical) are presented. Explicit results are obtained for a GaAs quantum wire.

We compare the results of the polaronic corrections with that of the exchange-correlation induced corrections. We found that they are comparable in order of magnitude, indicating that carrier-phonon interactions are more enhanced as the dimensionality reduces, and hence should be treated on an equal footing along with the carrier-carrier interactions. We make comparison with the polaronic corrections in two dimensional systems. Finally, we briefly discuss the renormalization due to confined phonons as well.

Keywords: Low dimensional electron gas, exchange-correlation, electron-phonon interaction, polarons, random-phase approximation, Hartree-Fock approximation, dielectric function.

Özet

DÜŞÜK BOYUTLU ELEKTRON-DEŞİK SİSTEMLERİNDE FONON RENORMALİZASYONU

Kaan Güven
Fizik Yüksek Lisans
Tez Yöneticisi: Doç. Dr. Bilal Tanatar
Eylül 1995

Düşük boyutlu yarı iletken yapılar, yoğun madde fiziğinin geniş bir araştırma alanını oluşturmaktadır. Son yıllarda yapılan çalışmaların önemli bir kısmı özellikle bireyakın boyutlu sistemler üzerinde yoğunlaşmaktadır. Boyutların indirgenmesiyle ortaya çıkan yeni fiziksel özellikler, bu sistemleri gelecekteki teknolojik uygulamalara potansiyel aday kılmaktadır. Kuram, "bir boyutlu" probleme uzun bir süreden beri tanıdık olmasına rağmen, bu yapıların hayata geçirilmesi ancak on yıl öncesine uzanmaktadır. Yeni üretim teknikleri deneysel çalışmalarda hızlı bir artışa sebep olurken, elde edilen deneysel verilerin sağlıklı bir şekilde yorumlanabilmesi için daha gerçekçi ve geniş kapsamlı bir kurama da ihtiyaç doğmuştur. Bu tez çalışması da sözkonusu ihtiyacın karşılanmasına bir katkıda bulunma amacı taşımaktadır.

Çalışma, boylamsal optik fononlarla etkileşen bireyakın boyutlu bir elektron-deşik sistemi üzerine kuruldu. Polaronik düzeltmelerin bant açıklığına ve yüktaşırların efektif kütlesine yaptığı katkılar, ve bu düzeltmelerin parçacık yoğunluğu, sıcaklık, kuantum boyutu etkilerine bağlılığı araştırıldı. Bu amaçla iki değişik metod kullanıldı; Dürtüsel kuram ve değişken prensibi kuramı. Bunlardan

ikincisi, dinamik perdeleme etkilerini gözönüne almayı sağlamaktadır. Elde edilen sonuçlar, düşük boyutlarda dinamik etkileşimlerin etkin olduğunu göstermiştir. Çok parçacık etkileşmeleri için temel bir nicelik olan dielektrik fonksiyonu, Hartree-Fock, rasgele faz ve yerel-alan düzeltmeleri gibi farklı yaklaşımlarda incelendi. Çeşitli sınırlandıcı potansiyeller model olarak sunuldu. Sayısal sonuçlar, bir GaAs kuantum teli örnek alınarak verildi.

Polaronik düzeltmeler için elde edilen sonuçlar, değişim-korelasyondan kaynaklanan düzeltmelerle karşılaştırılabilir düzeyde bulundu. Bu, düşük boyutlu sistemlerde yüktaşır-fonon etkileşimlerinin yüktaşır-yüktaşır etkileşmeleriyle aynı önemle ele alınması gerektiğini göstermektedir. Tezin sonunda, iki boyutlu sistemlerdeki fonon renormalizasyonu ile karşılaştırmalar yapılmakta ve sınırlandırılmış fononlarla yüktaşırların etkileşimlerine kısaca değinilmektedir.

Anahtar sözcükler: düşük boyutlu elektron sistemi, değişim-korelasyon, elektron-fonon etkileşimi, polaron, rasgele faz yaklaşımı, Hartree-Fock yaklaşımı, dielektrik fonksiyonu.

Acknowledgement

I would like to express my deep gratitude to Assoc. Prof. Bilal Tanatar for his supervision to my graduate study. I have enjoyed many fruitful discussions we had, which usually extended beyond philosophical concepts. I wish to thank him for his stimulation in a decisive yet a friendly way, and his invaluable comments for my graduate work.

I wish to thank Erkan Tekman for his assistance in writing the manuscript. I also appreciate discussions with other members of the Department of Physics, Bilkent University in the course of this study. Thanks folks!

There are friends, without their moral support these two years would have been hard. My special thanks are due to Özgür Müstecaphoğlu, my companion in Forgotten Realms, and to M. İhsan Ecemiş, my room-mate.

And the last but the most precious to me: Thank you, mom, dad, and Pelin!

Contents

List of Figures

Chapter 1

Introduction

Low dimensional semiconductor systems are an extensive research area in condensed matter physics. In particular, since the first suggestion by Sakaki[1] and the experimental realization by Petroff *et al.*[2] much effort has been devoted to the study of quasi-one dimensional (Q1D) structures in recent years. These systems, based on the confinement of the charge carriers in two transverse directions, exhibit new physical phenomena arising from the reduced dimensionality. From fundamental physics point of view, quantum wires are considered as examples of real one-dimensional Fermi gases, where one-dimensional electron dynamics can be studied in a controlled and quantitative manner. On the other hand, progress in the fabrication techniques such as molecular-beam epitaxy and lithographic deposition have made possible the production of such Q1D systems.[3–5] Quantum wires with active widths (along the plane of confinement) smaller than 300 Åand of negligible (less than 100 Å) thickness have been fabricated,[6,7] which allowed the attainment of the truly one-dimensional electric quantum limit, in the sense that only one quantum subband is populated by the electrons in the quantum wire. There is much excitement about the potential applications of these semiconductor quantum wires as high-speed transistors and efficient photodetectors and lasers. Hence there is a rapid growth in experimental research on these structures which, meanwhile, acts as a feedback on the theoretical studies. Our main motivation comes at this point that a more extensive and improved theoretical survey is

required to make a reliable comparison with the future experimental results. We restrict our attention to the many-body effects, and in particular to the interaction of charge carriers (i.e., electrons and holes) with phonons.

Formation of a dense electron-hole plasma in a semiconductor under intense laser excitation is a well known phenomenon. Typical densities of the plasma are of the order of 10^5 cm^{-1}. Because of the exchange and correlation effects, various single particle properties are affected, among which the most dramatic one is the band-gap renormalization (BGR). The exchange energy (or the Hartree-Fock energy), accounts for the correlations of the charge carriers due to the Pauli principle. The correlation energy is defined as the difference in energy between the Hartree-Fock value and any better calculation which takes the mutual interaction among the particles other than the Pauli principle, the Coulomb interaction for example. Both of these terms bring negative contributions to the self energies of electrons and holes. The change in the self energies lowers the conduction band and raises the valence band, thereby reducing the band-gap. It may be useful to give the definition of the BGR at this point.

$$\Delta E_g = E_g' - E_g = \Sigma_e(0) + \Sigma_h(0)\,,$$

where $\Sigma_{e,h}(0)$ are the electron and hole self-energies at the respective band edges. The density dependence of BGR is important to determine the emission wavelength of coherent emitters as being used in semiconductors.[8,9] Optical nonlinearities are associated with the BGR phenomenon because a substantial free carrier population can be induced by optical excitation and the consequent band-gap renormalization can affect the excitation process itself in turn. In 2D and 3D systems, the observed band-gaps are typically renormalized by ~ 20 meV within the range of plasma densities of interest. Band-gap renormalization as well as various optical properties of the electron-hole systems have been studied for bulk (3D) and quantum-well (2D) semiconductors,[10–15] providing generally good agreement with the corresponding measurements.[16–19] Density dependence of the BGR in Q1D systems was first considered by Benner and Haug[20] within the quasi-static approximation. Hu and Das Sarma[21] also calculated the BGR,

neglecting the hole population and considering an electron plasma confined in the lowest conduction subband only. Tanatar[22] studied the BGR in a Q1D electron-hole plasma investigating the density, temperature and quantum size dependences. Recently, Campos, Degani and Hipólito[23] presented the exchange and correlation effects in a Q1D electron gas using a self-consistent field method proposed by Singwi, Tosi and Sjölander.[24] Cingolani *et al.*[28,29] investigated the density dependence of a Q1D electron-hole plasma confined in GaAs quantum wires using luminescence spectra.

In low dimensional semiconductor structures, most often made of polar compound semiconductor materials, one has the additional complication of the long-range dipolar Fröhlich interaction between the charge carriers and the LO-phonons which also contributes to the renormalization processes. The band-gap and the carrier effective mass are renormalized by the absorption and emission of LO-phonons. It has been shown in Q2D systems that,[30] even for weakly polar materials such as GaAs this renormalization is present. Besides, several energy scales in the problem, namely the electron and hole Fermi energies, the dynamical plasma frequencies, and the LO-phonon energy become comparable which emphasizes the dynamical screening effects. We shall discuss the screening effects below in detail.

The coupling between charge carriers and LO-phonons introduces a new quasi-particle into the scheme, namely the polaron. It has been quite useful in describing the physical properties of carriers in ionic crystals and polar semiconductors. Earlier work on polarons deals with the interaction of a single charge carrier and a cloud of dispersionless virtual optical phonons, described by the Fröhlich Hamiltonian. Most of the polaron studies in low-dimensional systems have been done in the one-polaron limit. However, this approximation is rather difficult to justify because it contrasts with the real situation i.e., many carriers present in the system. One has to face a many-polaron system, which requires a many-body formulation treating the carrier-carrier and carrier- phonon interactions on an equal footing. Screening by free carriers (electrons in the conduction band and holes in the valence band) reduces the coupling between

carriers and LO-phonons. In the polaron picture, the BGR is associated with the polaronic self-energy. Similarly, the mass renormalization is due to the phonon cloud that the carrier has to carry with itself. Thus screening, by reducing the magnitude of the polaronic self-energy, acts to oppose the renormalization and tends to restore the gap to its unrenormalized value.

The effect of many electrons on the electron-phonon interaction in Q2D quantum wells were first investigated by Das Sarma.[31] He included screening effects, via Thomas-Fermi approximation and later[32] the static RPA (random-phase approximation). Lei[33] presented a full dynamical and finite temperature study of the electron self-energy in the presence of coupling with polar optical phonons in a GaAs-GaAlAs system. Wu, Peeters and Devreese[34,35] calculated the electron-phonon correction to the ground state energy of an interacting polaron gas within a dynamical screening scheme by taking into account the dielectric response at all frequencies. Das Sarma and Stopa[30] studied the phonon renormalization effects in Q2D wells. They employed the static approximation and the dynamical scheme mentioned above and presented explicit results for a GaAs system. Wendler[36,37] and later Jalabert and Das Sarma[38] re-investigated the influence of screening on the ground state properties of a many-polaron system in Q2D and in strictly two dimensions within the full RPA. Da Costa and Studart[39] presented a theoretical study of the coupled electron-phonon in a degenerate polar electron gas.

The study of the electron-phonon interaction in Q1D systems has started recently.[41–45] Campos, Degani, and Hipólito[46] calculated the electron phonon contribution to the ground-state energy of a Q1D gas of interacting polarons by using the self-consistent field approximation. Screening of the electron phonon interaction in Q1D semiconductor structures is investigated by Hai, Peeters and Devreese.[47]

In this work, we present the formulation and results on a Q1D electron-hole plasma interacting with bulk LO-phonons based on our studies.[50,51] The outline of the work will be as follows: In the next two chapters we will derive the two methods we have applied, namely the perturbation theory and the variational

theory. The theoretical results will be given in the corresponding chapters immediately, thereby making a comparison between the two methods. In the last chapter we summarize the results, and briefly discuss the renormalization effects due to confined phonons.

Chapter 2

Perturbation Theoretical Approach

In this chapter, our aim is to calculate the effects of static screening on polaronic corrections to the renormalization of band edges and carrier effective mass. The formulation is similar to that of Das Sarma and Stopa[30] which they have applied for the phonon renormalization effects in quantum wells. We extend it to include both electrons and holes, as is appropriate for a photoexcited intrinsic semiconductor.

The perturbative approach consists of evaluating the leading order electron (hole)–LO-phonon self energy. Electron (hole)–LO-phonon coupling in Q1D systems depends on the well width, free carrier density, and temperature. Screening and phonon occupancy are temperature dependent as well. Since the screening function (dielectric function) $\varepsilon(q)$ carries the dependence on these parameters, we pay attention to the formulation of $\varepsilon(q)$, and investigate different models : We employ the temperature-dependent, static, RPA dielectric function and address also the question of validity of using the plasmon-pole approximation to it. Furthermore, we attempt to include the vertex corrections in an approximate way.

2.1 Scaling properties

Das Sarma *et al.*[53] have found that, when the carrier density and the well width are expressed in terms of effective dimensionless variables by scaling them with the effective Bohr radius for the material, the dimensionless-band-gap renormalization expressed in units of effective Rydberg shows a universality, independent of the band- structure details of the material and dependent only on r_s, the dimensionless interparticle separation, and on the dimensionless well width. They further showed that this two-parameter universality can be reduced to an approximate one-parameter universality by choosing suitable quasi-two-dimensional Bohr radius and effective Rydberg as effective length and energy scaling units respectively. Since we are calculating the polaronic corrections to the band-gap renormalization, we express these corrections in the same convention modified for a Q1D electron-hole system to be consistent with the results for Q2D systems. The effective length scale appropriate for our electron-hole system is the quasi-one- dimensional excitonic Bohr radius, whereas the energy scale is chosen as the effective excitonic Rydberg. They are defined as

$$a^*_{ex} = \frac{1}{m_{red}e^2}, \qquad Ry^*_{ex} = \frac{e^2}{2a^*_{ex}},$$

respectively, where e is the electron charge and m_{red} is the reduced mass of the electron-hole pair ($m^{-1}_{red} = m^{-1}_e + m^{-1}_h$). We take the common physical constants $\hbar$ (Planck's constant), and k_B (Boltzmann constant) to be equal to unity.

2.2 Theory

For the two-component Q1D system consisting of electrons and holes, we consider a square-well of width a with infinite barriers. It may be built from a Q2D quantum-well (grown in the z-direction) by introducing an additional lateral confinement. We assume that effective mass approximation holds and for GaAs take $m_e = 0.067m$, and $m_h = 0.4m$, where m is the bare (free) electron mass. The effective Coulomb interaction between the charge carriers in their lowest subband

is given by[21] the average over the subband wave functions

$$V(q) = \frac{2e^2}{\epsilon_0} F(q)\,, \tag{2.1}$$

where ϵ_0 is the lattice dielectric constant and $F(q)$ is the form factor of the Q1D system defined for subsequent use. For the infinite well potential it is given by

$$F(q) = \int_0^1 dx\, K_0(qax) \left[2 - (1-x)\cos(2\pi x) + \frac{3}{2\pi}\sin(2\pi x)\right]\,, \tag{2.2}$$

in which $K_0(x)$ is the zeroth-order modified Bessel function of the second kind. It is evident that the well width dependence (i.e finite size quantum effects) enters through the form factor into the formalism. $V(q)$ is the bare interaction between the carriers. (see Appendix A.1)

2.2.1 Electron (hole) self-energy

We assume that the electron (hole)–LO-phonon interaction is expressed in terms of the Fröhlich Hamiltonian. For weakly polar semiconductors, where $\alpha_{e,h}$ is small, a systematic perturbation expansion in the coupling constant $\alpha_{e,h}$ is meaningful. We shall discuss two methods in this context: the *Brillouin-Wigner perturbation theory* (BWPT) and the *Rayleigh-Schrödinger perturbation theory* (RSPT). The equation for the energy spectrum E of a particle of momentum vector k is,

$$E = \epsilon(k) + \mathrm{Re}\left[\Sigma(k, E)\right]\,, \tag{2.3}$$

where $\Sigma(k, E)$ is the retarded self-energy, and $\epsilon(k) = k^2/2m$. In BWPT, the imaginary part of the self-energy is neglected and Eq.(2.3) is solved by an approximate self-energy expression in which first few terms are evaluated in the perturbation expansion of $\Sigma(k, E)$. The *Tamm-Dancoff approximation* (TD) is a special case of BWPT, where only the first term (the one-phonon term) is evaluated. In the Rayleigh-Schrödinger form of perturbation theory (also called *on the mass shell* perturbation theory) energy and momentum are no longer separate variables. In evaluating $\Sigma(k, E)$, the energy is set equal to $\epsilon(k)$, so the self-energy is just a function of one variable k or, equivalently $\epsilon(k)$.

The studies on the electron-phonon interaction contribution to the electron self-energy in 2D,[34,35] and 3D[39] have shown that RSPT works better than BWPT. The former of these studies is done in the one-polaron limit, whereas the latter and the recent one investigates a many-polaron problem in 3D. In the light of these conclusions, we base our formulation on RSPT.

The leading order polaronic self-energy for a Q1D system is given by[40]

$$\Sigma_{e,h}(k, i\xi_n) = -T \sum_{i\omega_n} \int_0^\infty \frac{dq}{2\pi} \frac{|M_{e,h}(q)|^2}{[\varepsilon(q, i\omega_n)]^2} G_{e,h}(k-q, i\xi_n - i\omega_n)\, D(q, i\omega_n)\,, \quad (2.4)$$

where T is temperature, $M_{e,h}(q)$ is the unscreened electron (hole)-phonon interaction strength,

$$|M_{e,h}(q)|^2 = \frac{2\omega_{LO}^2 \alpha_{e,h}}{\sqrt{2m_{e,h}\omega_{LO}}} F(q)\,, \quad (2.5)$$

and ξ_n and ω_n are the standard Matsubara frequencies. The Fröhlich coupling constant for electrons and holes is defined as

$$\alpha_{e,h} = \frac{1}{2}\left(\frac{1}{\epsilon_\infty} - \frac{1}{\epsilon_0}\right) \frac{e^2}{\omega_{\rm LO}} \sqrt{2m_{e,h}\omega_{\rm LO}}\,. \quad (2.6)$$

In Eq. (2.6), ϵ_∞ is the optical dielectric constant, $\omega_{\rm LO} = 36.5\,$meV is the bulk LO-phonon energy in GaAs.

$G_{e,h}(k-q, i\xi_n - i\omega_n)$ is the one-electron (hole) Green's function. In principle, it should be determined from the Dyson equation $G_{e,h}^{-1} = G_{0\,e,h}^{-1} - \Sigma_{e,h}$ where $G_{0\,e,h}(k, i\xi_n)$ is the non-interacting Green's function,

$$G_{0\,e,h}(k, i\xi_n) = [i\xi_n - E_{0\,e,h}(k)]^{-1}\,, \quad (2.7)$$

with $E_{0\,e,h}(k) = \epsilon_{0\,e,h}(k) - \mu_{e,h}$, where $\epsilon_{0\,e,h}(k)$ and $\mu_{e,h}$ are being the single (non-interacting) particle energy and the chemical potential for each species, respectively. Equation (2.4) along with the Dyson equation thus defines a set of coupled equations which should be solved self-consistently. In practice, however, one can substitute G_0 for G in Eq. (2.4) to obtain a rather good leading order self-energy correction for the polaron problem.

$D(q, i\omega_n)$ is the renormalized LO phonon propagator describing the plasmon-phonon coupling process. It is given by

$$D(q, i\omega_n) = D_0(q, i\omega_n) \left[1 - D_0(q, i\omega_n) \frac{|M_q|^2 \chi_0(q, i\omega_n)}{\varepsilon(q, i\omega_n)} \right] , \tag{2.8}$$

where D_0 defines the bare-phonon propagator. If one treats the LO-phonons without any dispersion, and take the phonon energy at a fixed $\omega_{\rm LO}$, it has the form

$$D_0(q, i\omega_n) = \frac{2\omega_{\rm LO}}{(i\omega_n)^2 - \omega_{\rm LO}^2} . \tag{2.9}$$

In general, the system under study involves three different fields, namely the electron (hole), phonon, and plasmon, that are coupled to each other. These processes are not quite important in describing the ground state of the system. We should note, however, that they play a fundamental role for the excitations of the system. So, we neglect the plasmon-phonon coupling, by using D_0 instead of $D(q, i\omega_n)$.

The electron (hole) dielectric function $\varepsilon(q, i\omega_n)$ contains all the information about screening. A full dynamic screening in the perturbation calculation is intractable, so we shall work with static screening, i.e. $\omega_n \to 0$. A detailed analysis of the dielectric function will be given in section (2.2.3).

Under these assumptions, the self energy expression can be written as

$$\begin{aligned} \Sigma_{e,h}(k, i\xi) &= \frac{2\alpha_{e,h}}{\pi} \frac{\omega_{\rm LO}^2}{\sqrt{2m_{e,h}\omega_{\rm LO}}} \int_0^\infty dq \, \frac{F(q)}{[\varepsilon(q,0)]^2} \\ &\times \left[\frac{n_0 + f_{e,h}(k-q)}{i\xi_n + \omega_{\rm LO} - E_{0\,e,h}(k-q)} + \frac{n_0 + 1 - f_{e,h}(k-q)}{i\xi_n - \omega_{\rm LO} - E_{0\,e,h}(k-q)} \right] . \end{aligned} \tag{2.10}$$

Here, n_0 and $f_{e,h}$ are the Bose (phonon) and Fermi occupancy factors respectively

$$\begin{aligned} n_0 &= \left[e^{\beta\omega_{LO}} - 1 \right]^{-1} \\ f_{e,h}(k) &= \left[1 + e^{\beta\epsilon_{0\,e,h}(k)} \right]^{-1} . \end{aligned} \tag{2.11}$$

We will show later that when the Fermi energy $E_F \ll \omega_{\rm LO}$, the Fermi occupancy effects will not be important, as in the case of two dimensional (2D) systems.[30]

To obtain the real part, we do the standard analytic continuation $i\xi_n \rightarrow \xi + i\eta$ with $\eta \rightarrow 0^+$. We also change the energy variable from ξ to ϵ, where $\epsilon = \xi + \mu_{e,h}$.

$$\begin{aligned} \mathrm{Re}\,\Sigma_{e,h}(k,\epsilon) &= \frac{2\alpha_{e,h}}{\pi}\frac{\omega_{\mathrm{LO}}^2}{\sqrt{2m_{e,h}\omega_{\mathrm{LO}}}}\int_0^\infty dq\,\frac{F(q)}{[\varepsilon(q,0)]^2} \\ &\times \left[\frac{n_0 + f_{e,h}(k-q)}{\epsilon + \omega_{\mathrm{LO}} - \epsilon_{0\,e,h}(k-q)} + \frac{n_0 + 1 - f_{e,h}(k-q)}{\epsilon - \omega_{\mathrm{LO}} - \epsilon_{0\,e,h}(k-q)}\right]. \end{aligned} \tag{2.12}$$

We make the usual assumption of parabolic bands, taking the electron and hole single particle energies to be $\epsilon_{0\,e,h}(k) = k^2/2m_{e,h}$. This should be justified for the GaAs example we consider in this work, but for certain semiconductors such as InSb, nonparabolicity effects would require higher-order corrections. In addition, we evaluate the electron (hole)-phonon self-energies on the mass shell ($\epsilon_{e,h} = k^2/2m_{e,h}$) to obtain the polaronic corrections at the band edge $[\mathrm{Re}\,\Sigma_{e,h}(0,0)]$

$$\begin{aligned} E_p = &-\frac{2\alpha_{e,h}}{\pi}\frac{\omega_{\mathrm{LO}}^2}{\sqrt{2m_{e,h}\omega_{\mathrm{LO}}}} \\ &\times \int_0^\infty dq\,\frac{F(q)}{[\varepsilon(q)]^2}\,\frac{(2n_0+1)(q^2/2m_{e,h}) + (2f_{e,h}(q)-1)\omega_{\mathrm{LO}}}{(q^2/2m_{e,h})^2 - \omega_{\mathrm{LO}}^2}. \end{aligned} \tag{2.13}$$

2.2.2 Polaron effective mass

The definition of the polaron effective mass (in the long-wavelength limit) is

$$\frac{1}{m_{e,h}^*} = \frac{1}{m_{e,h}} + \lim_{k\rightarrow 0}\frac{1}{k}\frac{\partial}{\partial k}\mathrm{Re}\,\Sigma_{e,h}(k, k^2/2m)\,. \tag{2.14}$$

For low temperatures ($T \leq 50\,\mathrm{K}$), we neglect the phonon occupancy, taking $n_0 \rightarrow 0$. The remaining integrand can be expanded in powers of k. Then, taking the derivative, and letting $k \rightarrow 0$, we obtain

$$\frac{1}{m_{e,h}^*} = \frac{1}{m_{e,h}} - \frac{\alpha_{e,h}}{m_{e,h}}\left[\frac{2}{\pi}\frac{\omega_{\mathrm{LO}}^2}{\sqrt{2m_{e,h}\omega_{\mathrm{LO}}}}\frac{2}{m_{e,h}}\int_0^\infty dq\,\frac{F(q)}{[\varepsilon(q)]^2}\,\frac{q^2}{[\omega_{\mathrm{LO}} + q^2/2m_{e,h}]^3}\right]. \tag{2.15}$$

The above expression yields in the weak coupling limit ($\alpha_{e,h} \rightarrow 0$)
$m_{e,h}^* \approx m_{e,h}(1 + \alpha C)$, where C is given by the expression inside the brackets in Eq. (2.15).

2.2.3 The dielectric function

A full treatment of the total dielectric function for the electron-hole system coupled to LO-phonons is very complicated. In general, the total dielectric function should be in the form

$$\varepsilon_t = \varepsilon_{e,h} + \varepsilon_{ph}\,, \tag{2.16}$$

where $\varepsilon_{e,h}$ and ε_{ph} are the electron (hole) and phonon dielectric functions respectively. We take $\varepsilon_{ph} = 0$ and make the so called ϵ_0 approximation which consists of replacing ϵ_∞ (high frequency dielectric constant) by ϵ_0 in the Coulomb potential (Eq. (2.1)). The rationale for this approximation is that the main effect of the high- frequency LO phonons is to screen the Coulomb interaction, which is suitably accounted for by the replacement of ϵ_∞ by ϵ_0. Das Sarma *et al.*[53] investigated the validity of the ϵ_0 approximation for the 2D and Q2D semiconductor quantum wells and concluded that, for weakly polar materials (e.g. GaAs, InAs, Ge, Si) the band-gap renormalization is very well approximated by ϵ_0 provided that the carrier densities do not reach very high values. This is because with increasing carrier density the Fermi energies become comparable to the LO-phonon energy which makes ϵ_0 approximation less appropriate. Since the density range of interest in our system satisfies the condition $E_F < \omega_{\rm LO}$, the use of ϵ_0 is reasonable.

So the total dielectric function reduces to carrier dielectric functions only. The definition is

$$\varepsilon^{-1}(q,\omega) = 1 + V(q)\chi(q,\omega)\,, \tag{2.17}$$

where $V(q)$ includes the carrier-carrier interactions only, and χ is the polarizability function of the charge carriers. In the Hartree-Fock approximation the bare (non-interacting) polarizability functions are used (we suppress the q and ω dependences):

$$\chi = \chi_0\,, \tag{2.18}$$

$$\varepsilon^{HFA} = \frac{1}{1 + V\chi}\,. \tag{2.19}$$

In the RPA, the polarizability function is

$$\chi = \frac{\chi_0}{1 - V\chi_0}, \tag{2.20}$$

which gives

$$\varepsilon^{RPA} = 1 - V\chi_0. \tag{2.21}$$

A further advance for ε^{RPA} includes the local field corrections

$$\chi = \frac{\chi_0}{1 - V[1 - G]\chi_0}, \tag{2.22}$$

where G is known as the local field factor. The corresponding form of the dielectric function is

$$\varepsilon^{LFC} = 1 - \gamma V\chi_0. \tag{2.23}$$

where γ is the vertex correction

$$\gamma = \frac{1}{1 + VG\chi_0}. \tag{2.24}$$

The unscreened limit is obtained by

$$\varepsilon(q, \omega) \to 1, \tag{2.25}$$

i.e., no interactions are taken into account. The above equations summarize the general form of the dielectric function in several approximations. For our system, we work in the static screening approximation, and employ the static RPA for the dielectric function

$$\varepsilon(q, \omega = 0, T) = 1 - V(q)\left[\chi_e(q, \omega = 0, T) + \chi_h(q, \omega = 0, T)\right], \tag{2.26}$$

where $V(q)$ is the Coulomb interaction between the charged particles, and $\chi_{e,h}(q, \omega = 0, T)$ are the finite-temperature static polarizabilities for electrons and holes. The form we use for $\varepsilon(q, 0)$ is appropriate for a photoexcited intrinsic semiconductor, since screening by electrons and holes are treated on an equal footing. In the case of doped n- and p-type semiconductors, screening by electrons

and holes should be considered separately. At zero temperature, the general form of the polarizability function for a Q1D electron (hole) gas is given by[54]

$$\chi(q,\omega) = \chi_1(q,\omega) + i\,\chi_2(q,\omega) \tag{2.27}$$

with

$$\begin{aligned} \chi_1(q,\omega) &= \frac{m}{\pi q}\ln\left|\frac{\omega^2-\omega_-^2}{\omega^2-\omega_+^2}\right|, \\ \chi_2(q,\omega) &= \begin{cases} -m/q & \text{if } \omega_+ > \omega > \omega_- \\ 0, & \text{otherwise} \end{cases} \end{aligned} \tag{2.28}$$

where $\omega_\pm = q^2/2m_{e,h} \pm k_F q/m_{e,h}$ and $k_F = \pi n_{e,h}/2$ is the Fermi wave vector (see appendix A.2). Since we are dealing with the case $N_e = N_h$, k_F is the same for both species. For the static case ($\omega = 0$), the imaginary part is zero. Note also that the real part diverges for $q = 2k_F$. We calculate the finite-temperature polarizabilities using the Maldague[55] approach starting from the zero-temperature Q1D polarizability of an electron gas

$$\chi_{e,h}(q,\omega=0,T) = \frac{m_{e,h}}{\pi q}\int_0^\infty dl\,\ln\left|\frac{y+\sqrt{l}}{y-\sqrt{l}}\right|\frac{1}{\cosh^2(x/2-l)}, \tag{2.29}$$

where $x = \mu_{e,h}/T$ and $y = q/4\sqrt{m_{e,h}T}$. Here $\mu_{e,h}$ are the chemical potentials for each species at finite temperature. (see appendix A.2)

In various applications, the dielectric function $\varepsilon(q)$ was further simplified by the plasmon-pole approximation to the following form[20]

$$\varepsilon(q) = 1 + \sum_{i=e,h}\frac{\omega_{p,i}^2}{(Nq^2/m_i\kappa_i) + (q^2/2m_i)^2}, \tag{2.30}$$

where the plasmon frequency for the Q1D[56] system is $\omega_{p,i}^2 = (N/m_i)V(q)$ (in the long-wavelength limit), and the screening parameter is $\kappa_i = \partial N/\partial\mu_i$. The plasmon-pole approximation consists of ignoring the weight of single-particle excitations and assuming that all the weight of the dynamic susceptibility $\chi_0(q,\omega)$ is at an effective plasmon energy ω_p.

To improve RPA, we include to effects of local field correction. Using Eq.(2.23) we account for the vertex corrections to $\lambda(q)$ in the mean-field sense. We use the equivalent of Hubbard approximation for $G(q)$ in one-dimension[57]

$$G(q) \approx \frac{1}{2}\frac{V(\sqrt{q^2+k_F^2})}{V(q)}. \tag{2.31}$$

The physical nature of the Hubbard approximation is such that it takes exchange into account and corresponds to using the Pauli hole in the calculation of the local-field correction between the particles of the same kind. Coulomb correlations are omitted. In this simple form, the static local-field factor $G(q)$ is temperature independent.

2.3 Results

2.3.1 Polaronic correction to the band edges

We first investigate the density dependence of the polaronic correction at low temperatures. Since the dielectric function $\varepsilon(q)$ of a Q1D system diverges at $2k_F$ and $T = 0$, we choose a small but finite temperature to work with. Figures 2.1 (a) and 2.1 (b) show the electron and hole polaron energies, respectively, as a function of the carrier density N for various well widths at $T = 5\,\mathrm{K}$. The solid curves in both figures, from top to bottom, indicate widths of $a = 500$, 250, and 100 Å. With increasing plasma density, the polaron energy decreases indicating the screening of the electron (hole)–LO-phonon interaction. On the other hand, the effect of the finite size of the quantum well is that the polaron correction decreases as the well width increases. Das Sarma and Stopa have shown[30] that in Q2D systems, the polaron energy drops off very rapidly as the well increases from 0 (strictly two dimensions) to 100 Å. It then continues to fall more slowly as the well thickness increases further. Although we do not show the strictly one-dimensional limit, the behavior is the same in Q1D systems. There is a tendency for higher densities to be slightly less affected by an increase in well width than

lower densities. This can be seen by recognizing that at higher densities the self-energy depends more strongly on coupling with shorter wavelength (higher q) phonons; the others being screened out. The form factor for finite well thickness affects most strongly those short wavelength phonons.

In order to see the influence of the Fermi occupancy factors, we also plot by dashed lines E_p, calculated without $f_{e,h}$ in Eq. (2.13). In the density range of interest, they are negligible small, except close to $N \sim 10^6\,\mathrm{cm}^{-1}$ both for electrons and holes. Since $E_F \sim k_F^2 \sim N^2$, it turns out that the condition $E_F << \omega_{LO}$ breaks down for $N > 10^6\,\mathrm{cm}^{-1}$. In other words, the carriers start to fill their next respective subbands which violates the extreme quantum approximation.

Also drawn in these figures by horizontal dotted lines are the unscreened energies. They are calculated using Eq. (2.13) with $\varepsilon(q) \to 1$, $n_0 \to 0$, and $f_{e,h} \to 0$. The no-screening limit depends only on the well width, and typical numbers are $E_p = -3.879$, -2.403, and -1.575 meV for well widths of $a = 100$, 250, and 500 Å, respectively, for the case of electrons. The corresponding values for holes are $E_p = -6.631$, -3.773, and -2.340 meV.

In Figs. 2.2(a) and 2.2(b), we show the effects of finite temperature on the polaronic correction to the band gap as a function of plasma density at $a = 100$ Å. The solid lines indicate, from top to bottom, $T = 5$, 100, and 300 K. We note that as the temperature increases, E_p also increases in magnitude. As a general trend, the phonon renormalization decreases for higher values of the carrier density, while its rate is temperature dependent. The dashed curves in Fig. 2.2 gives the BGR calculated within the plasmon-pole approximation to the dielectric function using the same parameters. We note that the temperature dependent plasmon-pole approximation yields considerably different results from the RPA. Das Sarma *et al.*[53] have found significant deviations of the plasmon-pole approximation from the full RPA result in two-dimensional (2D) quantum wells. Our calculations suggest increasing discrepancies between the full RPA and plasmon-pole approximation as T increases. The temperature dependence in the plasmon-pole approximation (Eq. (2.30)) mainly enters through the screening parameter κ and it is conceivable that differences originate from somewhat

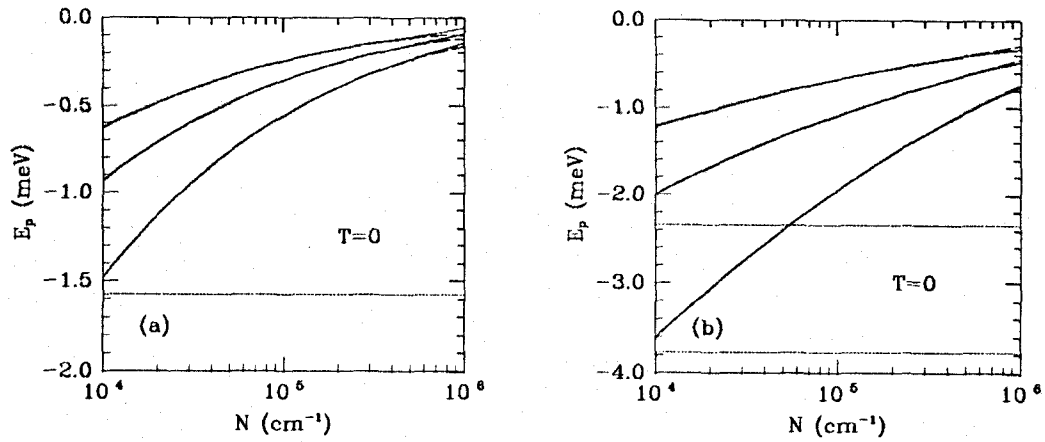

Figure 2.1: Density dependence of the polaron correction at different wire widths (a) Polaron correction to the conduction-band edge as a function of the carrier density N at $T = 5$ K. Solid (dashed lines from top to bottom are for well widths $a = 500$, 250, and 100Å, with (without) Fermi surface effects. The corresponding dotted lines indicate the unscreened limits (not all of them are in the ranges of the graphs). (b) Same for the valence-band edge.

different temperature dependences.

Having established the insignificance of the Fermi occupancy factors in the polaronic correction to the BGR in the density range of interest ($10^4 < N < 10^6\,\mathrm{cm}^{-1}$, we now turn to the temperature dependence of E_p. Fig. 2.3 shows the polaronic energy as a function of temperature. Fig. 2.3(a) is the conduction band correction for various carrier densities, in a quantum wire of well width $a = 200\,\text{Å}$. Solid lines from top to bottom are for $N = 10^4$, 10^5, and $10^6\,\mathrm{cm}^{-1}$, respectively. In Fig. 2.3(b), the same quantity is plotted for the valence band. At low temperatures, E_p is due mainly to virtual phonons, since n_0 (the average number of real phonons in the system) becomes vanishingly small as $T \to 0$.

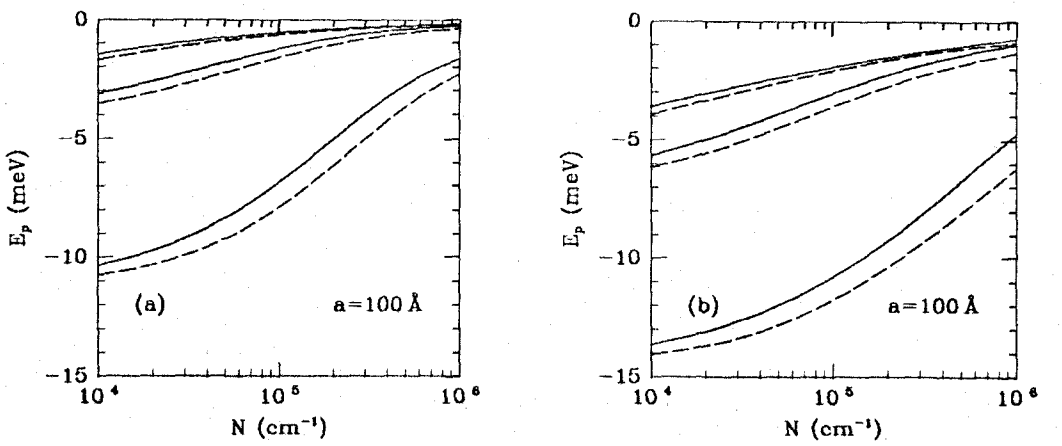

Figure 2.2: Density dependence of the polaron correction at different temperatures
(a) Polaron correction to the conduction-band edge as a function of the carrier density N for a quantum-well wire of width $a = 100\text{Å}$. The solid lines from top to bottom indicate $T = 0$, 100, and $300K$ calculated with full RPA, whereas the dashed lines are with the plasmon-pole approximation. (b) Same for the valence-band edge.

At higher temperatures, the average phonon number increases and emission and absorption of phonons contribute to E_p through the factors n_0 and $n_0 + 1$ in Eq. (2.13). The dashed lines in Fig. 2.3 are calculated without the phonon occupancy factors n_0 but we retain the dielectric function $\varepsilon(q)$. The difference between the dashed line and the corresponding solid line is a measure of the thermal phonon effects, which seem to be important for $T > 100\,\text{K}$. The dotted lines are calculated by setting $\varepsilon(q) = 1$ while keeping the phonon occupancy factors. In the no-screening limit this quantity is independent of the density.

For the most part, the dependence of self-energy on density and temperature merely reflects the dependence of screening on temperature and wavelength. Das

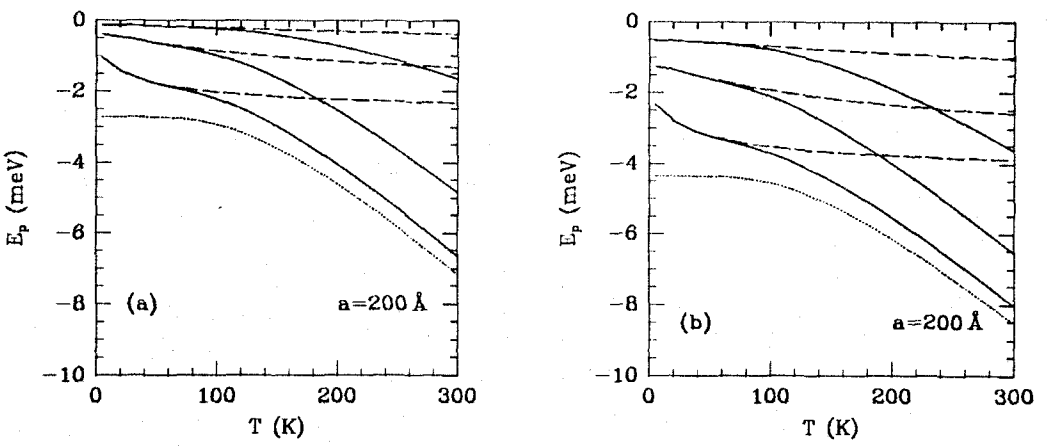

Figure 2.3: Temperature dependence of the polaron correction. (a) Correction to the conduction-band edge for a quantum-well wire of width $a = 200$ Å. The solid lines from top to bottom indicate $N = 10^6$, 10^5, and 10^4 cm^{-1}. The dashed lines show the effects of thermal phonons ($n_0 = 0$). The dotted line is calculated in the no-screening limit. (b) Same for the valence-band edge.

Sarma and Stopa have shown[30] that in Q2D wells, there is a competitive behavior of the screening and anti-screening effects on the polaron energy depending on the phonon wavelength at very low temperatures. The long wavelength (longer than the average interparticle separation $\sim 1/k_F$) phonons affect the electron more clearly at finite temperatures, and hence these renormalize the energy more effectively than at $T \approx 0$. However, for phonons whose wavelength is short according to the criteria given above, screening increases with temperature. At $T = 0$, other electrons are apparently "frozen out" of the region immediately surrounding a given electron. As thermal effects set in, the other electrons penetrate this region so that very short wavelengths are screened better at nonzero

temperatures. For low densities long-wavelength screening dominates so the self-energy decreases monotonically. At somewhat higher densities the anti-screening of short-wavelength starts to show up. In their work,[30] they have found that the anti-screening may lead even to a weak maximum near $T = 0$.

The foregoing results for the polaronic corrections at the conduction and valence band edges imply a total of $\sim 10\,\mathrm{meV}$ renormalization in the density range $10^4 < N < 10^6\,\mathrm{cm}^{-1}$ which is comparable to the exchange-correlation corrections.[28,21,20] The phonon renormalization effects become negligible for densities $N > 10^6\,\mathrm{cm}^{-1}$ irrespective of the quantum wire well width. We observe these effects also for a quantum wire of width $a = 500\,\text{Å}$ in Fig. 2.4. The solid lines in Fig. 2.4 are calculated with the RPA dielectric function, whereas in the dashed lines vertex corrections are included. Inclusion of the vertex corrections in the dielectric function through the local field factor brings about considerable changes in the theory of metals.

We observe that within the simple Hubbard approximation to $G(q)$, the BGR deviates only slightly from the RPA result. The difference in E_p with and without $G(q)$ is largely independent of temperature. We have also found good agreement for other values of the well width. These results suggest that the RPA is valid (in the range $10^4 < N < 10^6\,\mathrm{cm}^{-1}$) provided that the local-field factor we use is correct. In order to assess a more reliable measure of corrections beyond the RPA, better approximations to the local field factor $G(q)$ are needed.

2.3.2 Effective mass renormalization

The temperature dependent behavior of the mass renormalization is also a consequence of the dielectric function $\varepsilon(q,T)$, its main effect being to reduce the electron-phonon coupling. In the no-screening limit ($\varepsilon(q) \to 1$), the effective mass (renormalized mass) is independent of temperature and carrier density,

$$\frac{1}{m^*_{e,h}} = \frac{1}{m_{e,h}} - \frac{\alpha_{e,h}}{m_{e,h}} \left[\frac{2}{\pi} \frac{\omega^2_{\mathrm{LO}}}{\sqrt{2m_{e,h}\omega_{\mathrm{LO}}}} \frac{2}{m_{e,h}} \int_0^\infty dq\, F(q) \frac{q^2}{[\omega_{\mathrm{LO}} + q^2/2m_{e,h}]^3} \right] \quad (2.32)$$

which we write as $1/m^* = (1 - \alpha B)/m$. In the opposite limit of infinite screening ($\varepsilon \to \infty$) the electron (and hole) no longer couples to the phonon and there is

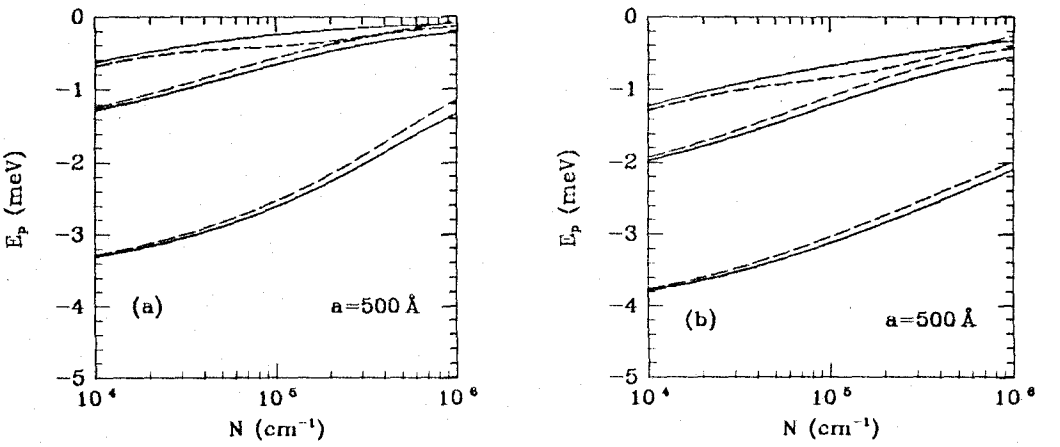

Figure 2.4: Vertex corrections
(a) For the conduction-band edge as a function of the carrier density N for a quantum-well wire of width $a = 500\mathring{A}$. The solid lines from top to bottom indicate $T = 0$, 100, and $300K$. The dashed lines are calculated with a dielectric function which includes the vertex corrections. (b) Same for the valence-band edge.

no mass renormalization, i.e., $m^*_{e,h} = m_{e,h}$. Thus m^* is bounded between the values $1/(1 - \alpha B)$ and 0.07 (0.4 for holes, and in units of bare electron mass). In Figs. 2.5(a) and 2.5(b) we display the per cent change in the band masses for electrons and holes, respectively, as a function of temperature. To illustrate the density dependence, we show (by solid lines) from top to bottom $N = 10^6$, 10^5, and $10^4\,\mathrm{cm}^{-1}$ for a quantum wire of well-width $a = 200\,\mathrm{\AA}$. Indicated by the dotted lines are the no-screening limit results discussed above. We observe that mass renormalization is rather large both for electrons and holes, $\sim 6\%$ and 10%, respectively.

We are not aware of any experiments to compare our results in quantum-well wires where the temperature dependence of the polaron mass is measured. In the

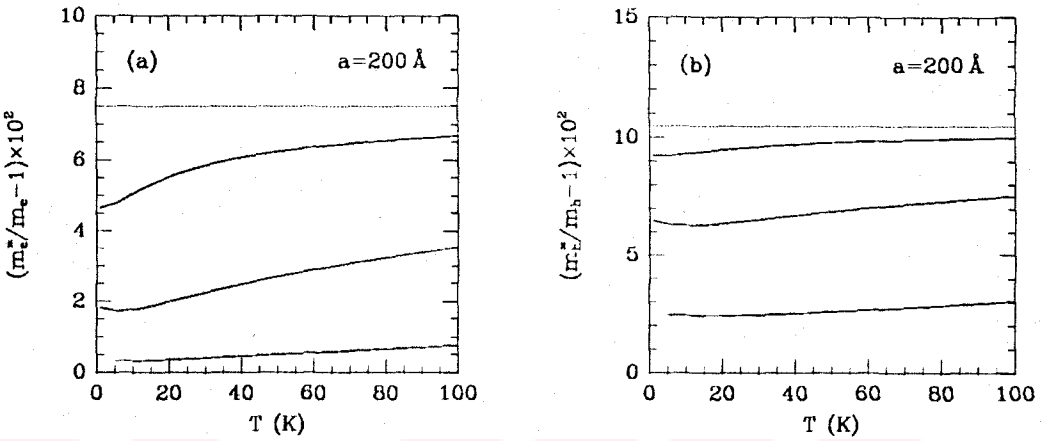

Figure 2.5: Effective mass renormalization
(a) At the conduction- band edge as a function of temperature for a quantum-well wire of width $a = 200\text{Å}$. The solid lines from top to bottom indicate $N = 10^6$, 10^5, and 10^4 cm^{-1}; the dotted line gives the no-screening limit. (b) Same for the valence-band edge.

case of 2D systems, Das Sarma and Stopa[30] found the mass renormalization to be rather small compared with the cyclotron resonance data. Since our analysis is along similar lines, we do not expect to obtain good agreement with the cyclotron resonance experiments. It remains an open problem to develop an adequate theory of screening of electron-phonon coupling in high magnetic fields.

Chapter 3

Variational Method

In low dimensional structures, the plasmon energy $\omega_{pl}(k)$ is generally much smaller than the LO-phonon energy ω_{LO}, in contrast to the situation in bulk, which may cause the dielectric function $\varepsilon(q,\omega)$ to behave very different at finite $\omega \sim \omega_{LO}$ from its $\omega = 0$ value (i.e., static value). Thus, the dynamical screening effects are expected to be important in low dimensional systems as pointed out by Lei.[33] In this chapter, we develop a variational formulation of the contribution of dynamical screening to the ground-state energy of an Q1D interacting electron-hole-phonon system. Our method is the generalization to two-component plasma of the variational calculation of polaron energy given by Lemmens *et al.*[58] The Q1D system we study contains electrons and holes at equal number density N, appropriate for an undoped, photoexcited semiconductor, and we consider the coupling with bulk LO-phonon modes. We compare our results with perturbation theory calculations performed in the previous chapter, to assess the validity of static approximation to the screening effects.

3.1 Theory

The specific model we use in our calculation for the Q1D, electron-hole fluid is developed by Das Sarma and Lai[59] and is applicable to the experimental realizations of semiconducting systems.[3] The charge carriers are assumed to be

in a zero thickness xy-plane with a harmonic (parabolic) confinement potential in the y-direction so that the subband energies are $\varepsilon_n = \Omega(n + 1/2)$ where Ω describes the strength of the confining potential. Again, we shall assume that both types of carriers are in their lowest subbands. This approximation will hold, as long as the subband separation remains much larger than the phonon energy in quantum wires and the thermal energy k_BT. The Coulomb interaction between the particles in our model Q1D system is given by[60] $(2e^2/\epsilon_0)F(q)$ where $F(q) = \frac{1}{2}\exp(b^2q^2/4)K_0(b^2q^2/4)$ in which $K_0(x)$ is the modified Bessel function, and ϵ_0 is the background dielectric constant (see appendix A.1). The characteristic length $b = 1/\sqrt{\mu\Omega}$, where μ is the reduced mass of the electron-hole pair, is related to the confining potential strengths of electrons and holes, and for simplicity we use throughout this paper the same value of b for both species. For more realistic calculations this restriction may easily be relaxed.

3.1.1 Lee-Low-Pines Transformation of the Hamiltonian

The total Hamiltonian for the interacting many-polaron system is given by

$$\begin{aligned}\mathcal{H} &= \sum_i \sum_k \frac{k^2}{2m_i} c^\dagger_{i,k} c_{i,k} + \sum_q \omega_{LO} a^\dagger_q a_q + \frac{1}{2}\sum_{i,j}\sum_{k,p,p'} V_{ij}(p') c^\dagger_{i,k+p'} c^\dagger_{j,p-p'} c_{j,p} c_{i,k} \\ &+ \sum_i \sum_q \left(M_{i,q} a^\dagger_q + M_{i,q} a^\dagger_{-q}\right) c^\dagger_{i,k+q} c_{i,k}\,, \end{aligned} \tag{3.1}$$

where i,j are the indices specifying the carrier type (i.e., electron or hole), $a^\dagger_q$ and a_q are the creation and annihilation operators for phonons with energy $\omega_{\rm LO}$ and wave number q, whereas $c^\dagger_k$ and c_k, respectively, create and annihilate an electron (hole) with wave vector k. $V_{ij}(q)$ is the Coulomb interaction between the particles. The electron (hole)-phonon interaction matrix element is given by[30,46,47] $|M_{i,q}|^2 = \left[2\alpha_i\,\omega^2_{\rm LO}/\sqrt{2m_i\omega_{\rm LO}}\right] F(q)$. So the first and second terms in the Hamiltonian are the free electron (hole) and phonon energies, respectively, whereas the third and fourth terms describe the carrier-carrier and carrier-phonon interactions.

We employ the Lee-Low-Pines unitary transformation[61] approach as developed by Lemmens *et al.*[58] and Wu *et al.*[34] in application to 3D and Q2D systems. This is a canonical transformation which belongs to the standard procedures to obtain variational estimates of the ground state energy of many polaron problem. In order to clarify the differences between this and the perturbation approach we review the essentials of the method. The Hamiltonian given by Eq. (3.1) is subjected to the similarity transformation

$$U = \exp Q\,, \tag{3.2}$$

where

$$Q = \sum_{i,k,q} f_{i,q}\,(a_q - a^\dagger_{-q})\,c^\dagger_{i,k}c_{i,k+q}\,. \tag{3.3}$$

The variational parameters $f_{q,i}$ are to be determined by minimizing the ground-state energy. The transformation of the operators can be calculated using the Baker-Hausdorff equation $e^{-A}Be^{A} = B + [B,A] + \frac{1}{2!}[[B,A],A] + \ldots$ The phonon operators a_q and $a^\dagger_q$ transform as displaced operators:

$$\begin{aligned} U^{-1}a_qU &= a_q - \sum_i f^*_{i,q}c^\dagger_{i,k}c_{i,k-q}\,, \\ U^{-1}a^\dagger_qU &= a^\dagger_q - \sum_i f_{i,q}c^\dagger_{i,k}c_{i,k+q}\,. \end{aligned} \tag{3.4}$$

The transformation of the electron (hole) operators gives

$$\begin{aligned} U^{-1}c_{i,k}U &= \exp\left[\sum_q f_{i,q}\,(a_q - a^\dagger_{-q})\right] c_{i,k}\,, \\ U^{-1}c^\dagger_{i,k}U &= c^\dagger_{i,k}\exp\left[-\sum_q f_{i,q}\,(a_q - a^\dagger_{-q})\right]\,. \end{aligned} \tag{3.5}$$

The transformation leads to the following form of the Hamiltonian:

$$U^{-1}\mathcal{H}U = H_{kin} + H_{ph} + H_{p-p} + H_{p-ph} + H_{ph-ph} + H_N\,. \tag{3.6}$$

H_{kin} is the kinetic energy of electrons and holes :

$$H_{kin} = \sum_i \frac{k^2}{2m_i}\,c^\dagger_{i,k}c_{i,k}\,. \tag{3.7}$$

H_{ph} is the free phonon part :

$$H_{ph} = \sum_{q} \omega_{\mathrm{LO}} a_q^{\dagger} a_q \,. \tag{3.8}$$

H_{p-p} describes the modified interaction between the charge carriers :

$$H_{p-p} = \frac{1}{2} \sum_{i,j} \sum_{q,p,p'} V_{ij}^{eff}\, c_{i,p+q}^{\dagger} c_{j,p'-q}^{\dagger} c_{j,p'} c_{i,p} \,, \tag{3.9}$$

where $V_{ij}^{eff}(q)$ is given by

$$V_{ij}^{eff}(q) = V_{ij}(q) - 2(M_{i,q}^{*} f_{j,q} + M_{i,q} f_{j,q}^{*} - \omega_{\mathrm{LO}} f_{i,q} f_{j,q}^{*}) \,. \tag{3.10}$$

H_{p-ph} is the carrier-phonon interaction :

$$\begin{aligned} H_{p-ph} = & \sum_{i,q} \left[(M_{i,q}^{*} - \omega_{\mathrm{LO}} f_{i,q}^{*}) a_q^{\dagger} + (M_{i,q} - \omega_{\mathrm{LO}} f_{i,q}) a_q \right] c_{i,k+q}^{\dagger} c_{i,k} \\ & + \sum_{i,k,q} \frac{k^2}{2m_i} \left(f_{i,q} a_q - f_{i,-q}^{*} a_{-q}^{\dagger} \right) c_{i,k}^{\dagger} c_{i,k+q} \,. \end{aligned} \tag{3.11}$$

H_{ph-ph} term gives the interaction between the phonons mediated by the charge carriers :

$$\begin{aligned} H_{ph-ph} = & \sum_{i,k} \sum_{q,q'} \frac{k^2}{2m_i} \left[(f_q f_{q'} a_q a_{q'} + f_{-q}^{*} f_{-q'}^{*} a_{-q}^{\dagger} a_{-q'}^{\dagger})\, c_{i,k}^{\dagger} c_{k+q+q'} \right. \\ & \left. + (f_q f_{q'}^{*} a_{q'}^{\dagger} a_q\, c_{k+q-q'} + f_q^{*} f_{q'} a_q^{\dagger} a_{q'}\, c_{k-q+q'}) \right] \,. \end{aligned} \tag{3.12}$$

The remaining term H_N contains only the number operator N_i :

$$H_N = \sum_{i,q} \left[(\omega_{\mathrm{LO}} + \frac{q^2}{2m_i}) f_{i,q}^{*} f_{i,q} - (M_{i,q}^{*} f_{i,q} + M_{i,q} f_{i,q}^{*}) \right] N_i \,. \tag{3.13}$$

In the next section we discuss the ground state energy of the transformed Hamiltonian.

3.1.2 The Variational Ground State Energy

For weakly polar materials the mean number of virtual phonons (i.e., the deformation of the lattice due to the presence of the charge carrier) in the polaron

cloud is small. Therefore, the phonon part of the ground state wave function can be described by by the vacuum state $|vac>$. The total wave function of the ground state is then

$$|\psi_{g.s.}>=|vac>\ |\psi_i>\,, \tag{3.14}$$

where $|\psi_i>$ are the ground state wave functions of electrons and holes. Within this ansatz, one can construct a reduced Hamiltonian which operates on the ground state of the charge carriers only :

$$\begin{aligned} H_{red} &= <vac|U^{-1}\mathcal{H}U|vac> \\ &= \sum_{i,k}\frac{k^2}{2m_i}c^\dagger_{i,k}c_{i,k}+\frac{1}{2}\sum_{i,j}\sum_{q,p,p'}V^{eff}_{ij}(q)\,c^\dagger_{i,p+q}c^\dagger_{j,p'-q}c_{j,p'}c_{i,p} \\ &\quad -\sum_{i,q}\left[(M^*_{i,q}f_{i,q}+M_{i,q}f^*_{i,q})+(\omega_{\rm LO}+\frac{q^2}{2m_i})f^*_{i,q}f_{i,q}\right]N_i\,. \end{aligned} \tag{3.15}$$

The minimum energy is found by taking the functional derivative of $<H_{red}>$ with respect to $f^*_{i,k}$'s and solving for $f_{i,k}$'s, which yields the following set of equations for $f_{i,k}$'s (we suppress the q-dependence of M_i and f_i)

$$\begin{aligned} (S_{11}\,\omega_{\rm LO}+q^2/2m_1)\ f_1+S_{12}\,\omega_{\rm LO}\,f_2 &= S_{11}M_1+S_{12}M_2\,, \\ (S_{22}\,\omega_{\rm LO}+q^2/2m_2)\ f_2+S_{12}\,\omega_{\rm LO}\,f_1 &= S_{22}M_2+S_{12}M_1\,, \end{aligned} \tag{3.16}$$

where $S_{ij}(q)$ are the static structure factors to be discussed below. Solving the above set of coupled equations for f_i, we obtain the polaronic contribution to the ground-state energy as

$$\begin{aligned} E_p = -\sum_q \{&S_{11}(M^*_1f_1+M_1f^*_1)+S_{12}(M^*_1f_2+M_1f^*_2+M^*_2f_1+M_2f^*_1) \\ &+S_{22}(M^*_2f_2+M_2f^*_2)\} \\ &+\sum_q\omega_{\rm LO}\,\{S_{11}f^*_1f_1+S_{12}(f^*_1f_2+f_1f^*_2)+S_{22}f^*_2f_2\} \\ &+\sum_q\left(\frac{q^2}{2m_1}f^*_1f_1+\frac{q^2}{2m_2}f^*_2f_2\right)\,. \end{aligned} \tag{3.17}$$

When the correlations between the electrons and holes are neglected, i.e., $S_{12}=0$, we obtain a simplified expression for the energy

$$E_p=-\left\{\sum_q|M_1|^2\frac{S^2_{11}}{\omega_{\rm LO}S_{11}+q^2/2m_1}+\sum_q|M_2|^2\frac{S^2_{22}}{\omega_{\rm LO}S_{22}+q^2/2m_2}\right\}\,, \tag{3.18}$$

as a sum of individual contributions of the plasma components. Furthermore, setting $S_{11} = S_{22} = 1$, amounts to the no-screening limit, and we recover the perturbation theory result.

3.1.3 Static Structure Factor

The structure factor describes the correlation between the interacting particles. It is a key quantity which has to be calculated in order to determine the screening properties of the polaron system. In most general form it is defined as

$$S(q,\omega) = \sum_n \left| < \psi_n | \rho_q^\dagger | \psi_0 > \right|^2 \delta(\omega - \omega_{n0}) \tag{3.19}$$

where ρ_q is the particle density operator, ψ_n are the exact wavefunctions of the system, and $\omega_{n0} = E_n - E_0$ is the difference in energy between the nth excited state and the ground state. $S(q,\omega)$ is a measure of the density fluctuation spectrum of the electron gas. There is a direct connection between this and the dielectric response function of the system.

$$S(q,\omega) = \frac{1}{\pi V(q)} \operatorname{Im}\left\{ \frac{-1}{\varepsilon(q,\omega)} \right\} . \tag{3.20}$$

For our system we shall use the static structure factor, with carrying the dynamic information as well. This is possible by using the following definition of the static structure factor

$$S(q) = \frac{1}{N} \int_0^\infty d\omega \, S(q,\omega) , \tag{3.21}$$

which may be called quasi-static structure factor. In evaluating the integral in Eq.(3.21), one has to be careful about the poles of the inverse dielectric function (Eq.(3.20)). There are two methods to overcome this difficulty. One is to calculate the single particle and the collective contributions separately[47]

$$S(q) = S_{eh}(q) + S_{pl}(q) . \tag{3.22}$$

The single particle contribution is calculated by using the RPA dielectric response function (Eq.2.21

$$S_{eh}(q) = \frac{1}{\pi N V(q)} \int_0^\infty d\omega \operatorname{Im}\left\{ \frac{-1}{\varepsilon^{RPA}(q,\omega)} \right\} , \tag{3.23}$$

whereas the plasmon contribution is calculated from[48]

$$S_{pl}(q) = \frac{-1}{\pi N V(q)} \frac{1}{\left[\frac{\partial}{\partial\omega}\mathrm{Re}\left\{\varepsilon(q,\omega)\right\}\right]_{\omega=\omega_{pl}}}. \tag{3.24}$$

The other method involves the extension of integral in Eq.(3.20) to the complex frequency domain and carrying the integration there.[49] We shall employ this method and discuss below. To establish the connection between the definition of the static structure factor and the formalism in the previous section, we rewrite the structure factor in the second quantization for the two component interacting system

$$S_{ij}(q) = \delta_{ij} + \frac{1}{N}\sum_{q,p,p'} < \psi_i|c^\dagger_{i,p+q}c^\dagger_{j,p'-q}c_{j,p'}c_{i,p}|\psi_j > \tag{3.25}$$

We consider two approximations in the evaluation of static structure factors $S_{ij}(q)$. In the first case, we use the Hartree-Fock (HF) approximation which has a simple form

$$S^{\mathrm{HF}}_{ij}(q) = \delta_{ij}\begin{cases} q/2k_F, & q < 2k_F \\ 1, & q \geq 2k_F \end{cases} \tag{3.26}$$

Note that in the HF approximation $S_{11} = S_{22}$ since we have equal number of electrons and holes, and $S_{12} = 0$. In the second case, we employ the RPA generalized to a two-component system.[62] The density-density response function of the system is expressed in matrix form

$$[\chi^{\mathrm{RPA}}(q,\omega)]^{-1} = \begin{pmatrix} [\chi^0_{11}(q,\omega)]^{-1} - V(q) & -V(q) \\ -V(q) & [\chi^0_{22}(q,\omega)]^{-1} - V(q) \end{pmatrix} \tag{3.27}$$

where $\chi^0_{ii}(q,\omega)$ is the Lindhard function for the ith component, i.e., non-interacting susceptibility. We calculate the corresponding static structure factors using[49]

$$S^{\mathrm{RPA}}_{ij}(q) = -\frac{1}{N}\int_0^\infty \frac{d\omega}{\pi}\,\chi^{\mathrm{RPA}}_{ij}(q,i\omega), \tag{3.28}$$

where the analytic continuation of the response function to the complex frequency plane and a subsequent Wick rotation of the frequency integral are used to incorporate the single-particle and plasmon contributions.

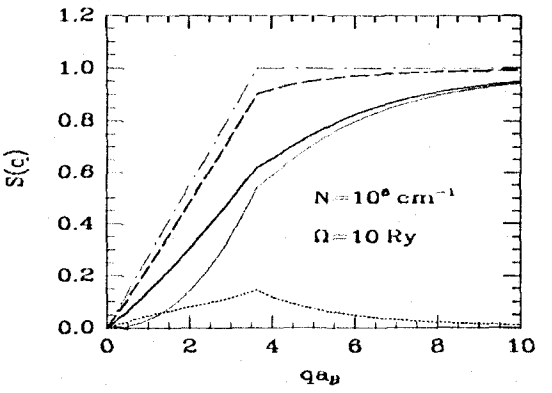

Figure 3.1: Static structure factors within RPA in a Q1D electron-hole system. Solid, dashed, and dotted lines indicate $S_{11}(q)$, $S_{22}(q)$, $S_{12}(q)$, respectively. The dash-dotted line is for the Hartree - Fock approximation. Thin solid line is the function $D(q) = S_{11}S_{22} - S_{12}^2$.

We again emphasize that, the static structure factors $S_{ij}(q)$ are obtained from the full frequency dependent response function $\chi(q,\omega)$ by integrating over all frequencies, thus they inherently carry dynamic information. For Q1D electron systems the collective excitations (plasmons) have a strong wave vector dependence without damping. Thus, along with the single-particle excitations, plasmons must also be taken into account in the calculation of $S_{ij}(q)$. The static structure factors, as set out above, determines the screening properties of the electron (hole)-phonon system. In Fig.3.1 we show the resulting partial structure factors in a two-component plasma for a typical density $N = 10^6\,\mathrm{cm}^{-1}$ and confinement energy $\Omega = 10\,\mathrm{Ry}$. Solid, dashed, and dotted lines indicate $S_{11}(q)$, $S_{22}(q)$, and $S_{12}(q)$, respectively, whereas dash-dotted line is the HF result. Also shown by the thin solid line is the quantity $D(q) = S_{11}(q)S_{22}(q) - S_{12}^2(q)$ as defined by Chakraborty.[63] It has been argued that $D(q)$ qualitatively resembles the static structure factor of a single species system at the same density.

3.2 Results

We illustrate our calculations of electron (hole)-phonon contribution to the ground-state energy of a quantum wire by choosing a GaAs system. The relevant parameters used in the calculations are $m_1 = 0.067m_e$, $m_2 = 0.5m_e$, for the electron and hole effective masses, respectively, $\alpha_1 = 0.07$, $\alpha_2 = 0.195$, for the electron-phonon and hole-phonon coupling constants, respectively, and $\omega_{\rm LO} = 36.5\,{\rm meV}$.

We show in Fig.3.2(a) the total polaronic contribution to the ground-state energy as a function of one-dimensional electron-hole plasma density N. The solid line represents the variational calculation employing the RPA structure factors to account for the screening effects. The variational calculation using the Hartree-Fock structure factors is indicated by the dashed line. For comparison we also show by the dotted line the result of a perturbative calculation.

We first note that both the variational RPA and the perturbative calculations exhibit considerable screening even at densities as low as $N \sim 10^5\,{\rm cm}^{-1}$. For the present choice of the confining potential energy ($\Omega = 10\,{\rm Ry}$) the unscreened polaron energy is about $-7\,{\rm meV}$. The Hartree-Fock approximation gives relatively small screening at low density, and in general it underestimates the screening effect. The perturbative calculation we have formulated in the previous chapter includes the static dielectric function $\varepsilon(q,0)$ through the renormalization of the electron (hole)-phonon interaction matrix element $|M_q|^2/[\varepsilon(q,0)]^2$. We use the $T = 0$, plasmon-pole approximation for $\varepsilon(q,\omega = 0)$ which includes the contribution of electrons and holes

$$\varepsilon(q,0) = 1 + \sum_{i=e,h} \frac{[\omega^i_{\rm pl}(q)]^2}{(q^2/2m_i)^2}\,, \tag{3.29}$$

where the Q1D plasmon frequency is $[\omega^i_{\rm pl}(q)]^2 = N\,(q^2/2m_i)\,V(q)$. As in the case of quantum-wells[30] (2D structures), static approximation overestimates the effects. We observe that going from the HF to RPA, the screening reduces the electron (hole)-phonon interaction appreciably for low carrier densities. It has been noted[30] that the static screening has a stronger effect in the renormalization

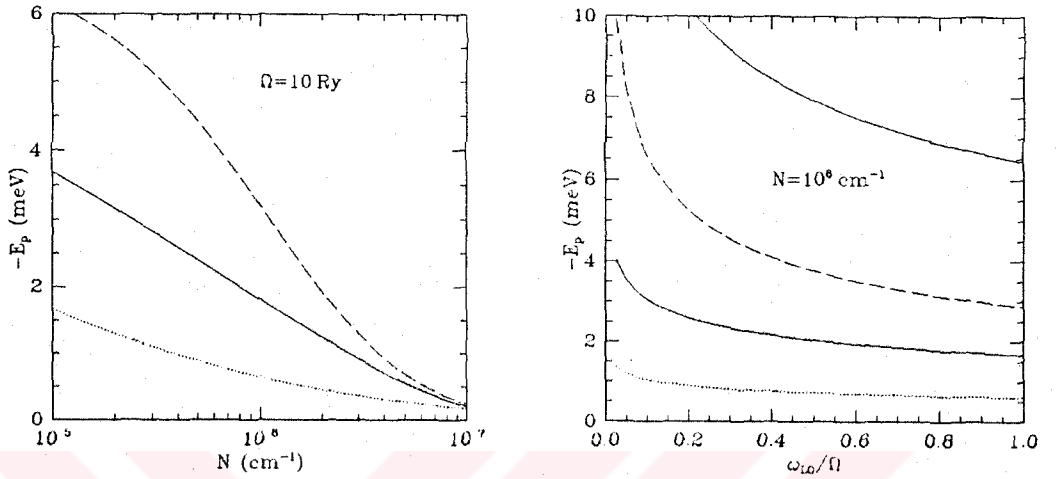

Figure 3.2: Polaronic contribution to the ground-state energy.
(a) Polaronic contribution to the ground-state energy for $\Omega = 10\,\mathrm{Ry}$ as a function of plasma density N; (b) for $N = 10^6$ cm^{-1} as a function of ω_{LO}/Ω. In both figures, the solid and dashed lines indicate the variational calculation using RPA and Hartree - Fock structure factors, respectively. The dotted line is for the perturbative calculation using the plasmon-pole approximation. The thin solid line in fig.(b) represents the unscreened limit.

(of polaron energy and mass) than the dynamic screening, because in the static approximation only the long-time response of the system is taken into account. Similar conclusions are drawn by Hai *et al.*[47] in a calculation that takes the dynamic screening effects into account for single-component Q1D systems.

In Fig.3.2(b), the confining potential energy dependence (or size dependence) of the polaronic contribution to the ground-state energy is illustrated. We show the results of various approximations as a function of ω_{LO}/Ω at a fixed plasma density $N = 10^6\,\mathrm{cm}^{-1}$. The solid and dotted lines represent the dynamical (variational, RPA), and static (perturbative, plasmon-pole approximation) screening calculations, respectively. We again observe that static approximation

overestimates screening effects in comparison to the dynamical approach. The variational calculation using the Hartree-Fock approximation to the structure factors (dashed line) appears to underestimate the screening effects especially for wide quantum wires (small Ω). The thin solid line indicates the unscreened polaron energy.

We have use the RPA to describe the many-body effects in the interacting system of electrons and holes rather uncritically. It may be argued that the attractive nature of the electron-hole interaction would make the two-component plasma structure factor calculations somewhat less reliable. It is known that the corrections to RPA become more important in lower dimensions than in 3D. Also, the RPA, although exact in the high density limit, fails to take the short-range electron correlations into account properly in lower density regime. For these reasons it would be worthwhile to investigate corrections to RPA through local-field factors using for instance the self-consistent field method of Singwi, Tosi, Land, and Sjölander.[24] The ground-state properties including the exchange-correlation effects in quantum-well wires beyond the RPA were recently studied by Campos *et al.*[23] To assess the importance of local-field corrections, we use the equivalent of Hubbard approximation in one-dimension given as

$$G_{ij}^{H}(q) \approx \frac{1}{2} \frac{V(\sqrt{q^2 + k_F^2})}{V(q)} \delta_{ij} \,, \tag{3.30}$$

which takes only the exchange effects into account, neglecting the Coulomb correlations. Figure 3.3 shows E_p as a function of plasma density for a quantum wire with $\Omega = 5\,\mathrm{Ry}$. The dashed line is calculated using the HF structure factors. The solid and dotted lines are with and without the local-field factor $G(q)$ included, respectively. We note that the local-field effects start to become important for densities less than $\sim 10^6\,\mathrm{cm}^{-1}$. In Chapter 2, we have shown that vertex corrections introduced within the perturbation theory did not affect E_p appreciably.

Our variational approach yields also effective interactions among the charge carriers modified by the interaction with phonons. In terms of the variational parameters f_i, they are given by Eq. (3.10). This result is the generalization of

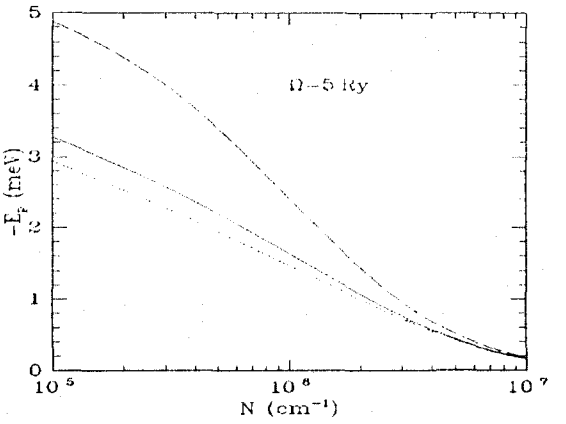

Figure 3.3: Effect of local-field correction on the polaron energy. The solid and dotted lines are calculated with and without $G(q)$, respectively, whereas the dashed line is the result of Hartree - Fock approximation.

the effective potential as derived by Lemmens *et al.*[58] and da Costa and Studart.[39] We display in Fig.3.4 the effective interactions for $N = 10^6\,\mathrm{cm}^{-1}$ and $\Omega = 10\,\mathrm{Ry}$ within the RPA. The solid and dotted lines are for V_{11}^{eff} and V_{22}^{eff}, and the dashed line is for V_{12}^{eff}. We have also shown, by the thin solid line, the bare Coulomb interaction for comparison. We find that the changes due to electron (hole)-phonon interactions are significant, but decrease with increasing width (small Ω) and increasing plasma density.

We point out that in the present method (variational) the polaronic energy in an electron-hole system is calculated at $T = 0$. It is possible to use a temperature dependent dielectric function $\varepsilon(q, T)$ within the perturbation theory approach.[30,50] For the variational calculation, not only the temperature dependent structure factors are necessary, but also the assumptions about the product form of the ground-state need to be justified.

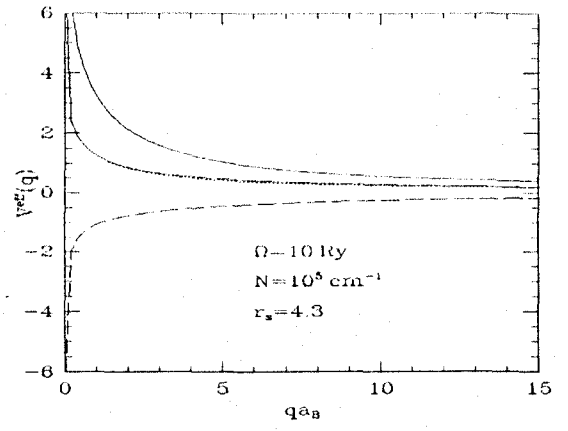

Figure 3.4: The effective interaction potential.
The effective interaction potential between the charge carriers at $N = 10^6$ cm^{-1} and $\Omega = 10$ Ry. Solid and dotted lines are for V_{11}^{eff} and V_{22}^{eff}, and the dashed line is for V_{12}^{eff}. The thin solid line is the bare Coulomb interaction.

3.3 Comparison with two-dimensional quantum-wells

The effects of screening on polaronic corrections to the effective band edges in a Q2D quantum-wells were considered by Das Sarma and Stopa.[30] They use the perturbative approach of evaluating the leading-order self-energy including static dielectric function, and a variational formalism involving the structure factor. Their approximation amounts to the 2D version of our simplified expression given in Eq.(3.18) It is of interest to apply the full dynamical screening effects within the variational approach to quantum-well structures. Fig.3.5 shows the results of our dynamically screened calculation for a strictly 2D system, for which the Coulomb interaction is taken to be $v(q) = 2\pi e^2/q$. The solid and dashed lines indicate the HF and RPA, respectively, for the total (electrons and holes) polaronic correction to the ground-state energy. We observe qualitatively similar

features to the Q1D case, in that, the RPA yields more screening than the HF approximation. The dotted line appearing in Fig.3.5 is for the statically screened perturbative calculation. At zero temperature, the static dielectric function for a 2D system is independent of density. Note that the 2D screening wave vector is given by $q_s = 2m\epsilon^2/\epsilon_0$. Thus, we have a constant line which nevertheless exhibits considerable screening (over screening) as noted by Das Sarma and Stopa.[30] Deviations from the constant behavior could be attributed to finite temperature effects. The dash-dotted line in Fig.3.5(a) is evaluated with the aid of Eq.(3.18) when the correlations between electrons and holes are neglected. We find that omitting $S_{12}(q)$ in Eq.(3.17) affects the polaronic contribution to the energy considerably.

We next study the effects of finite well width on the energy E_p. Assuming only the lowest subband is occupied both in conduction and valence bands, we use the form factor[30,64]

$$F(q) = \frac{8}{(q^2a^2 + 4\pi^2)} \left[\frac{3}{8}qa + \frac{\pi^2}{qa} - \frac{4\pi^2(1 - e^{-qa})}{q^2a^2(q^2a^2 + 4\pi^2)} \right],$$

where a is the well width. In Fig.3.5(b), we display the polaronic contribution to the ground-state energy as a function of quantum-well width at a typical plasma density $N = 5 \times 10^{11}\,\mathrm{cm}^{-2}$. We note that the screening effects dominate as the well width is increased. Similar conclusions may be drawn from the calculations of Das Sarma and Stopa.[30] A more complete many-body calculation within the perturbation theory of the band-gap renormalization which includes the electron-electron and electron-phonon interactions for semiconductor quantum-wells were performed by Das Sarma *et al.*[53]

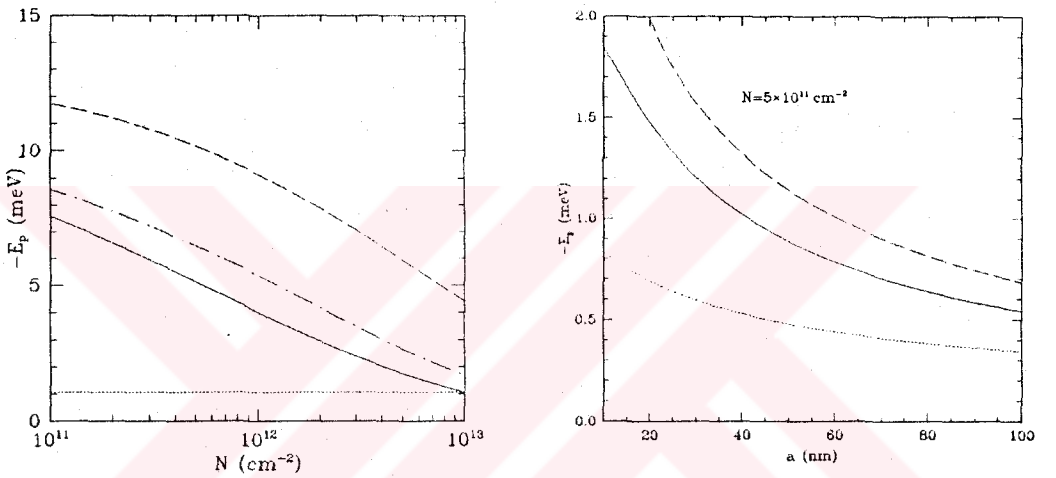

Figure 3.5: Polaronic contribution to the ground-state energy in 2D systems. (a) Polaronic contribution in a strictly 2D system as a function of plasma density. (b) The size dependence of the polaronic contribution in a quantum-well structure. In both figures the solid and dashed lines are calculated using Hartree - Fock and RPA structure factors, respectively . The dotted line is the result of perturbative calculation including static screening. The dash-dotted line in fig.(b) shows the variational approach in RPA without the cross term $S_{12}(q)$.

Chapter 4

Discussion and Conclusion

We have presented two different methods to investigate the polaronic corrections on the single particle properties in a quasi-one-dimensional electron-hole system. A strictly competitive approach in comparing the results of these methods would not be true, since they provide complementary information as well. The variational method emphasized the importance of the dynamical nature of screening, whereas it is the perturbational approach where the temperature dependence can be analyzed easily. In addition to that, since no equivalent canonical transformation has been developed to calculate the effective masses in variational method, our results for the polaronic mass renormalization rely on the static screening treatment of the many polaron system as discussed in Chapter 2.

The overall results have shown that the polaron self-energy is comparable to the exchange-correlation effects in order of magnitude. A direct consequence of this result is that in low dimensional structures, the interaction between the charge carriers and phonons and among the charge carriers themselves should be treated on an equal footing. The confinement potential determines the carrier phonon interaction directly but the general trends obtained for the carrier density and screening dependence should be valid irrespective of the details of the model chosen. We have verified this by using two different models, namely, the infinite well and the parabolic confinement potentials.

The dependence of the polaronic correction on relevant parameters are

discussed in detail in the previous chapters, so we briefly summarize them here:

- Screening by free carriers strongly affect the carrier-phonon interaction, hence the polaron self-energy. As the plasma density increases, the polaron self-energy decreases.
- The quantum size effects of the system plays an important role. The polaron energy decreases with increasing "width" of the quantum wire.
- Temperature is a restoring parameter for the polaron energy. This is mainly due to the fact that at finite temperatures the mean number of phonons increases which brings an enhancement to the polaron energy.
- The renormalization of the polaron effective mass can be explained in the same terms in which we understand the behavior of the polaron self-energy.

It may be useful to review the main assumptions for the construction of the many-body system. We have taken a two-component plasma consisting of electrons and holes of equal number density and focused on the interaction of this two-component plasma with bulk LO-phonons. First, we assumed that the electron-hole plasma is in equilibrium, which can be justified, since the laser pulse durations are much longer than the particle relaxation rates in these semiconductor structures under study. Second,the subband structure is ignored by taking the extreme quantum limit, in which the chemical potential of each carrier type lies in the lowest respective subband. This, however, puts limitations on the range of carrier number density, temperature, and the effective width of the wire from which the first two control the level of the chemical potential, and the last one determines the subband separation. On the other hand, the existence of LO-phonons put another criteria for the subband separation, that it must be larger than the phonon energy ω_{LO}, so that electrons (holes) cannot scatter into higher subbands via their interaction with phonons. The energy and the effective mass of an electron in a quantum wire including the subband effects were calculated in the presence of electron–LO-phonon interaction by Degani and Hipólito.[65,66] Ryan and Reinecke[67] presented a multisubband formulation for an

electron-hole system. Their work was obtaining the band-gap renormalization due to exchange-correlation effects, including the intersubband and intrasubband interactions.

Our work is based on a photoexcited intrinsic semiconductor, hence the number of electrons and holes are the same. The extension to doped semiconductors should be straightforward. We note however, that taking the hole density equal to zero does not reflect the real situation because all experiments measuring band-gap shifts involve creation or annihilation of electron-hole pairs which result in a renormalization of the valence band. We further ignored the degenerate nature of the valence band, approximating it by the simple parabolic dispersion.

Along with the LO-phonon coupling one may include the coupling to confined phonons and interface phonons as well. However, there is no experimental evidence of the coupling of the interface optical phonons to the confined electrons as pointed out by Das Sarma and Mason.[64] Secondly, in heterostructure type systems consisting of two lattice matched semiconductors (e.g. GaAs and AlGaAs) with rather similar lattice dielectric properties, the existence of purely interface phonon modes is rather unlikely. The interface phonon modes will have exponentially decaying amplitudes into the wire, which makes them negligible unless the wire is too narrow. We shall discuss the coupling to confined phonons in the next section.

4.1 Phonon confinement effects

Fasol *et al.*[68] have presented evidence of phonon confinement in low dimensional structures. Phonon confinement causes changes on the carrier-phonon interaction, modifying properties like scattering rate and relaxation rates from those in the bulk case. Considerable work has been done[71,72] on the role of confined phonon modes in the hot-electron relaxation phenomena in semiconductor quantum wells. To obtain the confined phonon modes, the three dimensional Fröhlich Hamiltonian is subjected to boundary conditions at the interfaces.

There are two different macroscopic approaches to phonon confinement: the electrostatic or the slab modes[71] and the mechanical or the guided modes.[72] They differ essentially in the way the boundary conditions are applied. In the slab model the electrostatic potential vanishes at the boundaries, whereas in the guided model it is the electric field. Stroscio[69] has applied the dielectric continuum model to describe the the confined LO-phonons in rectangular quantum wires. On the other hand Rücker *et al.*[70] presented a calculation of the polar electron–LO-phonon interaction in GaAs/AlAs quantum wells, based on a fully microscopic approach for the phonon spectra. According to their comparison, some of the macroscopic models lead to acceptable predictions, whereas some of them are completely inconsistent with the microscopic results. It turns out that the correct use of the dielectric boundary conditions is crucial for the applicability of the macroscopic models to polar electron-phonon scattering. They concluded that, the assumption of unmodified bulk phonons may provide resonable results, and pointed out that an accurate description of the phonons is necessary when one is interested in the contribution of individual modes, e.g., for the interpretation of results of time-resolved spectroscopies.

Recently, we have presented a preliminary investigation of the contribution of confined phonon modes to the ground-state energy of a Q1D electron-phonon system, and in particular the effects of screening on this contribution.[52] The polaron energy is calculated variationally incorporating the dynamic screening effects and it is found that the confined phonon contribution is comparable to that of bulk phonons in the density range $N = 10^4 - 10^7$ cm^{-1}.

Appendix

A.1 Effective Coulomb Interaction

Here, we give the form factor of a quasi-one-dimensional system for several confinement potentials. In the first two models that we consider, the wire is constructed as follows: We take a strictly two-dimensional electron-hole plasma in the $x - y$ plane and introduce an additional confinement in the y direction. So the wire has zero "thickness" but finite "width". The reason that we neglect the finite size effects along the z direction is just for simplicity and will not lead to a qualitative change in the obtained results. Besides, this assumption can be justified, because, at this stage the technology for confining the charge carriers to two dimensions is much more advanced than technology for confining the electrons along and additional direction. For example by modulation doping, the electrons can be confined in the z direction on the order of less than 100 Å, whereas the confinement in y direction is approximately 300 Å, leading to at least an order of magnitude difference in the energy-level spacings of the y and z directions. The last model we present is a quantum wire with a circular cross-section.

We based our formulation mainly on the RPA. Consequently, the effective potential we use in our calculations is the bare Coulomb potential given by Eq.(2.1). Campos, Degani, and Hipólito[23] have calculated the effective Coulomb potential in rectangular GaAs quantum well-wire using the self-consistent field approximation (so called the STLS approximation), which incorporates the

exchange-correlation effects. There, the effective potential is given by

$$\phi(q) = V(q) + \frac{1}{2\pi nq} \int_0^\infty dk\,[S(k) - 1][(q+k)V(q+k) + (q-k)V(q-k)]\,,$$

which implies that the RPA results correspond to the zeroth-order approximation where $\phi(q)$ is taken as the bare Coulomb interaction potential $V(q)$. Their results[23] indicate that RPA underestimates and the HFA overestimates the short range correlation effects.

From electrodynamics point of view, the presence of other charge carriers should be taken into account when calculating the effective potential acting on an individual charge carrier. This amounts to a numerical solution of the Schrödinger equation coupled to the Poisson equation, which has been considered in some studies[25–27] concerning the self-consistent electronic subband structure of a quantum wire.

Below, we represent the general part of the derivation. The one-electron (hole) wavefunction is given by

$$\psi_{q,n}(x,y,z) = \frac{1}{\sqrt{V}}\, e^{iqx}\, \xi_n(y)\, \delta(z)\,, \qquad \text{(A.1.1)}$$

where V is the volume of the wire, q is the wave vector in x direction, $\xi_n(y)$ is the bound state wave function for the nth subband associated with the quantized y motion. The wave function will not have z component, but it is shown here by a delta function for completeness. We will drop that term henceforth. The explicit form of $\xi_n(y)$ is obtained from Schrödinger Equation

$$\left[-\frac{1}{2m}\frac{\partial^2}{\partial y^2} + V(y)\right]\, \xi(y) = E_n\, \xi(y)\,, \qquad \text{(A.1.2)}$$

with a choice of the confining potential $V(y)$. The matrix elements of the Coulomb interaction are given by

$$V_{klmn}(q-q') = \int_{-\infty}^{\infty}\int_{-\infty}^{\infty}\int_{-\infty}^{\infty}\int_{-\infty}^{\infty} dx\,dx'\,dy\,dy' \times \left[\psi^*_{q,k}(x,y)\,\psi^*_{q',l}(x',y')\,v(x-x',y-y')\,\psi_{q,m}(x',y')\,\psi_{q',n}(x,y)\right]\,, \qquad \text{(A.1.3)}$$

where $v(x-x', y-y')$ is given by

$$v(x-x', y-y') = \frac{e^2/\epsilon_0}{\sqrt{(x-x')^2+(y-y')^2}}. \tag{A.1.4}$$

At this step it is possible to carry out the integration over the variable x in Eq.(A.1.3). This leads to one-dimensional Fourier transformation of $v(x-x', y-y')$:

$$\tilde{v}(q, y-y') = \frac{2e^2}{\epsilon_0}\int_{\infty}^{\infty} dt\, \frac{e^{iqt}}{\sqrt{t^2+(y-y')^2}}, \tag{A.1.5}$$

where we let $t \equiv x - x'$. The integral in Eq.(A.1.5) can be represented by $K_0(x)$, the modified Bessel function of the second kind, of order zero.[73]

$$\tilde{v}(q, y-y') = \frac{2e^2}{\epsilon_0} K_0\left[|q(y-y')|\right]. \tag{A.1.6}$$

Hence, the form factor is given by

$$F_{klmn} = \int_{-\infty}^{\infty}\int_{-\infty}^{\infty} dy\, dy' K_0\left[|q(y-y')|\right]\, \xi_k(y)\, \xi_l(y')\, \xi_m(y')\, \xi_n(y), \tag{A.1.7}$$

where we have used Eq.(2.1) along with Eq.(A.1.3).

Infinite well confinement

We take the confinement potential in y direction as infinite well

$$V(y) = \begin{cases} 0, & -a/2 \le y \le a/2 \\ \infty, & \text{otherwise.} \end{cases} \tag{A.1.8}$$

There are two families of solutions for the subband wavefunctions

$$\xi_n(y) = \begin{cases} \sqrt{\frac{2}{a}} \sin\left(n\pi\frac{y}{a}\right), & n \text{ even} \\ \sqrt{\frac{2}{a}} \cos\left(n\pi\frac{y}{a}\right), & n \text{ odd} \end{cases} \tag{A.1.9}$$

where n denotes the subband indices. The subband energies are

$$E_n = \frac{\pi^2 n^2}{2\mu a^2}. \tag{A.1.10}$$

The explicit form of $F_{klmn}(q)$ can be found for any values of the subband indices in a straightforward manner. Since we are dealing with the extreme quantum limit, we take k,l,m,$n = 1$. Using Eq.(A.1.9) in Eq.(A.1.7) gives

$$F(q) = \left(\frac{2}{a}\right)^2 \int_{-a/2}^{a/2}\int_{-a/2}^{a/2} dy\, dy'\, K_0\left[|q(y-y')|\right] \left(\cos\frac{\pi y}{a}\,\cos\frac{\pi y'}{a}\right)^2 . \qquad \text{(A.1.11)}$$

A further change of integration variables $x = (y - y')/a$, $x' = (y + y')/a$ yields

$$F(q) = 2\int_0^1 dx \int_0^{1-x} dx'\, K_0(|qax|)\,(\cos\pi x + \cos\pi x')^2 . \qquad \text{(A.1.12)}$$

Then, taking the integral over x' gives Eq.(2.2).

Parabolic confinement

The confinement potential is given by

$$V(y) = \frac{1}{2}\mu\Omega^2 y^2 , \qquad \text{(A.1.13)}$$

where μ is the reduced mass, Ω is the strength of the confining potential. The envelope functions in y direction are given by,

$$\xi_n(y) = \left[\frac{1}{2^n n!\sqrt{\pi}b}\right]^{\frac{1}{2}} e^{-y^2/2b^2} H_n(y/b) . \qquad \text{(A.1.14)}$$

The subband energies are

$$E_n = \Omega(n + \frac{1}{2}) . \qquad \text{(A.1.15)}$$

Here, $b = 1/\sqrt{\mu\Omega}$ is the characteristic length of the parabolic potential, and $H_n(y)$ is the Hermite polynomial. The interesting point in parabolic confinement is that, one can obtain the form factor in closed form. Hu and O'Connell[60] presented the analytical calculation for the Coulomb matrix elements in Q1D system using the harmonic (parabolic) confinement potential. They have given detailed calculations for some of the diagonal part of the Coulomb matrix, for both the intrasubband ($nn = k = l = m = n$) and the intersubband ($nn = k = l$, $nn' = m = n$) interaction.The underlying algebra is quite complicated, thus we

cite the general form only and give the explicit form factor for the lowest subband case which is our main interest.

$$F_{\{N\}}(q) = \begin{cases} \sum_{s=0}^{N/2} B_s^{\{N\}} \frac{\sqrt{2}\pi}{qb} e^{q^2b^2/4} W_{-s,0}(\frac{1}{2}q^2b^2), & N\,, \text{even} \\ 0, & N\,, \text{odd} \end{cases} \tag{A.1.16}$$

where $\{N\}$ is a collective index representing $N = k + l + m + n$, $W_{\lambda\mu}(x)$ is the Whittaker function, $B_s^{\{N\}}$ are the coefficients. For $N = 0$, the result is[60]

$$F(q) = e^{q^2b^2/4} K_0(q^2b^2/4)\,, \tag{A.1.17}$$

as given in section 3.1. We also note that, in the long wavelength limit ($bq \rightarrow 0$), the typical logarithmic divergent behavior of the strictly one-dimensional Coulomb interaction can be obtained for this form factor,

$$F(q \rightarrow 0) \rightarrow -\ln(bq)\,. \tag{A.1.18}$$

Cylindrical confinement

In this case, the wire is taken to be along the x direction with a circular cross section of radius R. We choose the confinement potential as

$$V(r) = \begin{cases} 0\,, & r < R \\ \infty\,, & R < r \end{cases} \tag{A.1.19}$$

where $r = \sqrt{y^2 + z^2}$. The radial part of the wavefunction can be obtained by solving the Schrödinger equation in polar coordinates,

$$-\left(r\frac{\partial}{\partial r}r\frac{\partial}{\partial r} + V(r)\right)\xi(r) = E\,\xi(r)\,, \tag{A.1.20}$$

which gives

$$\xi_{mn}(r) = \frac{1}{R}\left[\frac{J_m(j_{mn}\frac{r}{R})}{J_{m+1}(j_{mn})}\right]\,, \tag{A.1.21}$$

where j_{mn} is the nth zero of the Bessel function $J_m(x)$. The subband energies are given by

$$E_{mn}(0) = \frac{1}{2\mu}\left[\frac{j_{mn}}{R}\right]^2\,. \tag{A.1.22}$$

The total wavefunction has the following form

$$\psi_{m,n,k} = \frac{1}{\sqrt{\pi L R}} \left[\frac{J_m(j_{mn}\frac{r}{R})}{J_{m+1}(j_{mn})} \right] e^{im\phi} e^{ikx} . \qquad \text{(A.1.23)}$$

The integral in Eq.(A.1.7) has, to our knowledge, no analytical form. Gold and Ghazali[57] presented analytical results for the form factor by employing approximate wavefunctions for the ground state and first excited state,

$$\xi_{01}(x) = \sqrt{3}\,(1 - x^2)\,, \qquad \text{(A.1.24)}$$

$$\xi_{\pm 11}(x) = \sqrt{12}\,(x - x^3)\,, \qquad \text{(A.1.25)}$$

with the corresponding subband energies,

$$E_{01}(0) = \frac{6}{2\mu R^2}\,, \qquad \text{(A.1.26)}$$

$$E_{11}(0) = \frac{16}{2\mu R^2}\,, \qquad \text{(A.1.27)}$$

where $x = r/R$. We skip the details of the calculation and give the final result[57]

$$F(q) = \frac{36}{(qR)^2} \left[\frac{1}{10} - \frac{2}{3(qR)^2} + \frac{32}{3(qR)^4} - \frac{64}{(qR)^4} I_3(qR) K_3(qR) \right] . \qquad \text{(A.1.28)}$$

Here, $I_n(x)$ and $K_n(x)$ are the modified Bessel functions of the first and second kind respectively. The definitions of all the special functions employed in this appendix may be found in Abramowitz and Stegan.[74]

A.2 Polarizability Function in 1D

The polarizability function (also known as the density-density response function) is obtained from the dynamical evolution of a charge density fluctuation. In the RPA, one obtains the unperturbed (free electron) polarizability function for an electron plasma as

$$\chi(q,\omega) = \sum_k \frac{f_{k-q} - f_k}{\omega + \epsilon_{k-q} - \epsilon_k + i\eta}\,, \qquad \text{(A.2.1)}$$

where f_k is the Fermi distribution function, $\epsilon_k = k^2/2m$ is the free electron energy. We write the polarizability function as $\chi = \chi_1 + i\chi_2$, in terms of real and imaginary parts. Eq.A.2.1 can be rewritten as

$$\chi(q,\omega) = \sum_k f_k \left[\frac{1}{\omega - (\epsilon_{k+q} - \epsilon_k) + i\eta} - \frac{1}{\omega - (\epsilon_k - \epsilon_{k-q}) + i\eta} \right] . \qquad \text{(A.2.2)}$$

Using the Dirac identity given below, one can obtain the real and imaginary parts explicitly

$$\frac{f(z)}{z - z_0 \mp i\eta} = \mathcal{P}\left(\frac{f(z)}{z - z_0}\right) \pm i\pi f(z)\delta(z - z_0) , \qquad \text{(A.2.3)}$$

$$\chi_1(q,\omega) = 2\mathcal{P} \int_{-\infty}^{\infty} \frac{dk}{2\pi} f_k \left[\frac{1}{\omega - (\epsilon_{k+q} - \epsilon_k)} - \frac{1}{\omega - (\epsilon_k - \epsilon_{k-q})} \right] , \qquad \text{(A.2.4)}$$

$$\chi_2(q,\omega) = -2\pi \int_{-\infty}^{\infty} \frac{dk}{2\pi} f_k \left[\delta(\omega - \epsilon_{k+q} + \epsilon_k) - \delta(\omega - \epsilon_k + \epsilon_{k-q}) \right] , \qquad \text{(A.2.5)}$$

where the overall factor 2 is due to spin states.

$T = 0$ case

At $T = 0$ K, the Fermi distribution function is $f_k = \theta(|k_F| - k)$. Using this and the explicit forms of ϵ_k's, Eq.(A.2.4) becomes

$$\chi_1 = \frac{1}{\pi} \int_{-k_F}^{k_F} dk \left[\frac{1}{\omega - \left(\frac{kq}{m} + \frac{q^2}{2m}\right)} - \frac{1}{\omega - \left(\frac{kq}{m} - \frac{q^2}{2m}\right)} \right] . \qquad \text{(A.2.6)}$$

Upon integration we get the final form as[54]

$$\chi_1 = \frac{m}{\pi q} ln \left| \frac{\omega^2 - \omega_-^2}{\omega^2 - \omega_+^2} \right| , \qquad \text{(A.2.7)}$$

where

$$\omega_\pm = \left| \frac{k_F q}{m} \pm \frac{q^2}{2m} \right| . \qquad \text{(A.2.8)}$$

The imaginary part of χ becomes

$$\chi_2 = -\int_{-k_F}^{k_F} dk \, [\delta(\omega - \omega_+) - \delta(\omega - \omega_-)] \qquad \text{(A.2.9)}$$

$$= \begin{cases} -\frac{m}{q}, & \omega_- < \omega < \omega_+ \\ 0, & \text{otherwise} \end{cases} \qquad \text{(A.2.10)}$$

(A.2.11)

$T > 0$ case

Maldague[55] has given a derivation of the finite temperature polarizability function and represented explicit results for 2D electron gas. We apply the derivation given there for 1D case. For finite temperatures the Fermi function is given by $f_k = \{1 + \exp[(\epsilon_k - \mu)/T]\}^{-1}$ where $\epsilon_k = k^2/2m$, and μ is the chemical potential. To evaluate Eq.(A.2.1) we use the following integral representation of the Fermi function.

$$f_k = \int_0^\infty d\mu'\, \theta(\mu' - \epsilon_k)\, \frac{1}{4T\cosh^2[(\mu - \mu')/2T]}\,, \tag{A.2.12}$$

where $\theta(\mu' - \epsilon_k)$ is the zero-temperature Fermi function with Fermi energy μ'. Replacing in Eq.(A.2.1) and performing the integral over μ' first, we find

$$\chi(q,\omega;T,\mu) = \int_0^\infty d\mu'\, \chi(q,\omega;0,\mu')\, \frac{1}{4T\cosh^2[(\mu - \mu')/2T]}\,, \tag{A.2.13}$$

where $\chi(q,\omega;0,\mu')$ is the zero temperature polarizability function. By using Eqs.(A.2.7) and (A.2.9) we can obtain the real and imaginary parts for the finite temperature polarizability function explicitly.

$$\chi_1(q,\omega;T,\mu) = \frac{m}{\pi q}\int_0^\infty dt\, ln\left|\frac{\omega^2 - \frac{4Tq}{m}\left(y + \sqrt{t}\right)}{\omega^2 - \frac{4Tq}{m}\left(y - \sqrt{t}\right)}\right| \frac{1}{\cosh^2\left(t - \frac{\mu}{2T}\right)}\,, \tag{A.2.14}$$

where $y = q/4\sqrt{mT}$. Setting $\omega = 0$ leads to the static limit and we obtain Eq.(2.29). The imaginary part becomes

$$\chi_2(q,\omega;T,\mu) = \frac{m}{\pi}\left\{f\left[\frac{1}{4x}(\omega + x)^2\right] - f\left[\frac{1}{4x}(\omega - x)^2\right]\right\}\,. \tag{A.2.15}$$

where $x = q^2/2m$ and f is the Fermi function. We also note that one can make use of the Kramers-Kronig relations to obtain the real part from the imaginary part and vice versa.

$$\chi_1(q,\omega) = \frac{2}{\pi}\int_0^\infty d\omega'\, \chi_2(q,\omega)\mathcal{P}\frac{\omega'}{\omega'^2 - \omega^2}\,. \tag{A.2.16}$$

Bibliography

[1] H. Sakaki, Japanese Journal of Applications **19**, L735 (1988).

[2] P. M. Petroff, A. C. Gossard, R. A. Logan, and W. W. Wiegmann, " Toward quantum well wires - Fabrication and optical properties", Applied Physics Letters **41**, 635 (1982).

[3] T. Demel, D. Heitmann, P. Grambow, and K. Ploog, "Far-infrared response of one-dimensional electronic systems in single layered and double layered quantum wires", Physical Review B **38**, 2732 (1988).

[4] J. Christen, M. Grundmann, E. Kapon, E. Colas, D. M. Hwang, and D. Bimberg, "Ultrafast carrier capture and long recombination lifetimes in GaAs quantum wires grown on nonplanar substrates", Applied Physics Letters **61**, 67 (1992).

[5] A. Schmeller, A. R. Gõni, A. Pinczuk, J. S. Weiner, J. M. Calleja, B. S. Dennis, L. N. Pfeiffer, and K. W. West, "Inelastic light scattering by spin-density, charge-density, and single particle excitations in GaAs quantum wires", Physical Review B **49**, 14778 (1994).

[6] J.M. Calleja, A.R.Gõni, B.S.Dennis, J.S.Weiner, A. Pinczuk, S. Schmitt-Rink, L. N. Pfeiffer, K. W. West, J. F. Müller, A. E. Rückenstein, "Large optical singularities of the one-dimensional electron-gas in semiconductor quantum wires", Solid State Communications **79**, 911 (1991).

[7] A.S. Plaut, H.Lage, P.Grambow, D.Heitmann, K. Volklitzing, K. Ploog, "Direct magnetooptical obxervation of a quantum confined one-dimensional

electron-gas", Physical Review Letters **67**, 1642 (1991); *ibid.* A. R. Goñi, A. Piczuk, J. S. Weiner, J. M. Calleja, B. S. Dennis, L. N. Pfeiffer, K. W. West, "One-dimensional plasmon dispersion and dispersionless intersubband excitations in GaAs quantum wires", **67**, 3298 (1991).

[8] S. Schmitt-Rink, D. S. Chemla, and D. A. B. Miller, "Linear and nonlinear optical-properties of semiconductor quantum wells", Advances in Physics **38**, 89 (1989).

[9] R. Cingolani and K. Ploog, "Frequency and density dependent radiative recombination processes in III-V semiconductor quantum-wells and superlattices", Advances in Physics **40**, 535 (1991).

[10] H. Haug and S. Schmitt-Rink, "Electron theory of the optical-properties of laser-excited semiconductors", Progresses in Quantum Electronics **9**, 3 (1984).

[11] H. Haug and S. Schmitt-Rink, "Basic mechanisms of the optical nonlinearities of semiconductors near the band edge", Journal of Optical Society of America B **2**, 1135 (1985).

[12] S. Schmitt-Rink, C. Ell, S. W. Koch, H. E. Schmidt, and H. Haug, "Subband-level renormalization and absorbative optical bistability in semiconductor multiple quantum well structures", Solid State Communications **52**, 123 (1984).

[13] H. Haug, and S. W. Koch, "Semiconductor laser thoery with many-body effects", Physical Review A **39**, 1887 (1989).

[14] C. Ell, R. Blank, S. Benner, and H. Haug, "Simplified calculations of the optical-spectra of two-dimensional and 3-dimensional laser-excited semiconductors", Journal of Optical Society of America B **6**, 2006 (1989).

[15] C. Ell, H. Haug, and S. W. Koch, "Many-body effects in gain and refractive-index spectra of bulk and quantum-well semiconductor-lasers", Optics Letters **14**, 356 (1989).

[16] G. Tränkle, C.Ell, A.Forchel, G. Griffiths, H. Haug, H. Krömer, E. Lach, F. Scholz, S. Subbanna, G.Weimann, "General relation between band-gap renormalization and carrier density in two-dimensional electron-hole plasmas", Physical Review B **36**, 6712 (1987); *ibid.* G. Tränkle, C. Ell, A. Forchel, H. Haug, H. Leier, G. Weimann, "Dimensionality dependence of the band-gap renormalization in two-dimensional and 3-dimensional electron-hole plasmas in GaAs", Physical Review Letters **58**, 419 (1987).

[17] G. Bongiovanni and J. L. Staehli, "Properties of the electron-hole plasma in GaAs-(Ga, Al)As quantum wells - The influence of the finite well width", Physical Review B **39**, 8359 (1989).

[18] C. Weber, C.Klingshirn, D.S.Chemla, D.A.B. Miller, J. E. Cunningham, C. Ell, "Gain measurements and band-gap renormalization in GaAs / $Al_xGa_{1-x}As$ multiple quantum-well structures", Physical Review B **38**, 2748 (1988).

[19] V. D. Kulakovskii, E.Lach, A.Forchel, D. Grutzmacher, "Band-gap renormalization and band-filling effects in a homogeneous electron-hole plasma in $In_{0.53}$ $Ga_{0.47}$ As /InP single quantum wells", Physical Review B **40**, 8087 (1989).

[20] S. Benner and H. Haug, "Plasma density dependence of the optical-spectra for quasi-one-dimensional quantum-well wires", Europhysics Letters **16**, 579 (1991).

[21] B. Y. K. Hu and S. Das Sarma, "Many-body properties of a quasi-one-dimensional semiconductor quantum wire", Physical Review Letters **68**, 1750 (1992); *ibid.* "Many-body exchange-correlation effects in the lowest subband of semiconductor quantum wires", Physical Review B **48**, 5469 (1993).

[22] B. Tanatar, "Band-gap renormalization in quasi-one-dimensional electron-hole systems", *unpublished.*

[23] V. B. Campos, M. H. Degani, and O. Hipólito, "Exchange and correlation effects in a semiconductor quantum-well wire", Superlattices and Microstructures **17**, 85 (1995); A. N. Borges, M. H. Degani, and O. Hipólito, Superlattices and Microstructures **13**, 375 (1993); *ibid* **17**, 85 (1995).

[24] K. S. Singwi, M. Tosi, R. H. Land, and A. Sjölander, Physical Review B **176**, 589 (1968).

[25] S.A.Laux an F.Stern, Applied Physics Letters **49**, 91 (1986).

[26] S.A.Laux, D.J.Frank, and F.Stern, "Quasi-one-dimensional electron states in a split-gate GaAs / AlGaAs heterostructure", Surface Science **196**, 101 (1988).

[27] C.R.Proetto, "Self-consistent electronic structure of a cylindrical quantum wire", Physical Review B **45**, 11911 (1992).

[28] R. Cingolani, R. Rinaldi, M. Ferrara, G. C. La Rocca, H. Lage, D. Heitmann, K. Ploog, and H. Kalt, "Band-gap renormalization in quantum wires", Physical Review B **48**, 14331 (1993).

[29] R. Cingolani, H. Lage, L. Tapfer, H. Kalt, D. Heitmann, and K. Ploog, "Quantum confined one-dimensional electron-hole plasma in semiconductor quantum wires", Physical Review Letters **67**, 891 (1991).

[30] S. Das Sarma and M. Stopa, "Phonon renormalization effects in quantum wells", Physical Review B **36**, 9595 (1987).

[31] S. Das Sarma, "Polaron effective mass in GaAs heterostructure", Physical Review B **27**, 2590 (1983); **37**, 4034 (E) (1985).

[32] S. Das Sarma and B. A. Mason, "Screening of polar interaction in quasi-two-dimensional semiconductor microstructures", Physical Review B **31**, 5536 (1985); **32**, 2656 (E) (1985).

[33] X. L. Lei, "Dynamical screening and electron self-energy in the presence of polar interaction in quasi-2D heterostructures", Journal of Physics C: Solid State Physics **18**, L713-L735 (1985).

[34] W. Xiaoguang, F. M. Peeters, and J. T. Devreese, "Screening of the electron-phonon interaction in GaAs heterostructures", Physica Status Solidi (b) **133**, 229 (1986); *ibid* Physical Review B **31**, 3420 (1985).

[35] F. M. Peeters and J. T. Devreese, "Energy-levels of two-dimensional and 3-dimensional polarons in a magnetic field", Physical Review B **31**, 3689 (1985).

[36] L. Wendler, R. Haupt, and V. G. Grigoryan, "Intersubband mixing of coupled plasmon-phonons in double heterostructures", Physica Status Solidi (b) **149**, K123 (1988).

[37] L. Wendler, "Landau-damped collective excitations of the quasi-two-dimensional polaron gas in double heterostructures", Solid State Communications **65**, 1197 (1988).

[38] R. Jalabert and S. Das Sarma, "Many-polaron interaction effects in two dimensions", Physical Review B **39**, 5542 (1989).

[39] W. B. da Costa and N. Studart, "Interacting many-polaron system in degenerate semiconductors", Physical Review B **47**, 6356 (1993).

[40] G.D.Mahan, *Many Particle Physics*, (Plenum, New York, 1981), pp. 487-499.

[41] N. C. Constantinou and B. K. Ridley, "Effects of finite well depth on polar optical phonon scattering rates in cylindrical quantum well wires', Journal of Physics Condensed Matter **1**, 2283 (1989).

[42] X. G. Wu, "Dynamical conductivity of a quasi-one-dimensional electron-gas", Physical Review B **39**, 8062 (1989).

[43] M. H. Degani and G. A. Farias, "Anisotropic polarons near interfaces of polar semiconductors", Physical Review B **42**, 11950 (1990).

[44] M. H. Degani and O. Hipólito, "Interaction of phonons with electrons in GaAs quantum wires", Solid State Communications **65**, 1185 (1988).

[45] M. H. Degani, "Energy-momentum relation for polarons in quantum well wires", Physical Review B **40**, 1937 (1989).

[46] V. B. Campos, M. H. Degani, and O. Hipólito, "Many-polaron interaction effects in GaAs-GaAlAs quantum-well wires", Solid State Communications **79**, 473 (1991).

[47] G. Q. Hai, F. M. Peeters, J. T. Devreese, and L. Wendler, "Screening of the electron-phonon interaction in quasi-one-dimensional semiconductor structures", Physical Review B **48**, 12016 (1993).

[48] D.Pines, *Elementary Excitations in Solids*, (Addison-Wesley, USA, 1963).

[49] L.Zheng and A.H.MacDonald, "Correlation in double-layer two dimensional electron-gas systems: Singwi-Tosi-Land-Sjölander theory at $B = 0$", Physical Review B **49**, 5522 (1994).

[50] K. Güven and B. Tanatar, "Phonon renormalization effects in photoexcited quantum wires", Physical Review B **51**, 1784 (1995).

[51] K. Güven and B. Tanatar, "Variational approach for phonon renormalization effects in photoexcited quantum wires and quantum wells", *to be published.*

[52] B. Tanatar and K. Güven, "Phonon confinement and screening effects on the polaron energy in quantum wires", Semiconductor Science and Technology **10**, 803 (1995).

[53] S. Das Sarma, R. Jalabert, and S. R. E. Yang, "Band-gap renormalization in quasi-two dimensional systems induced by many-body electron-electron and electron-phonon interactions", Physical Review B **39**, 5516 (1989); *ibid* **41**, 8288 (1990).

[54] P.F.Williams and A.N.Bloch, Physical Review B **10**, 1097 (1974).

[55] P. Maldague, "Many-body corrections to the polarizability of the two-dimensional electron gas", Surface Science **73**, 296 (1978).

[56] Q. Li and S. Das Sarma, "Plasmon excitations in one-dimensional lateral-quantum-wire superlattices", Physical Review B **41**, 7626 (1990).

[57] A. Gold and A. Ghazali, "Exchange effects in a quasi-one dimensional electron-gas", Physical Review B **41**, 7626 (1990).

[58] L. F. Lemmens, J. T. Devreese, and F. Brosens, "On the ground state energy of a gas of interacting polarons", Physica Status Solidi (b) **82**, 439 (1977).

[59] S. Das Sarma and W. Y. Lai, "Screening and elementary excitations in narrow-channel semiconductor microstructures", Physical Review **32**, 1401 (1985).

[60] G. Y. Hu and R. F. O'Connell, "Electron-electron interactions in a quasi-one-dimensional electron systems", Physical Review B **42**, 1290 (1990).

[61] T. D. Lee, F. E. Low, and D. Pines, "The motion of slow electrons in a polar crystal", Physical Review B **90**, 297 (1953).

[62] P. Vashishta, P. Bhattacharyya, and K. S. Singwi, Physical Review B **10**, 5108 (1974).

[63] T. Chakraborty, "Structure of binary boson mixtures at $T = 0$ K", Physical Review B **26**, 6131 (1982); *ibid.* "Ground-state correlations in the layered electron-hole liquid", Physical Review B **29**, 3975 (1984).

[64] S.Das Sarma and B.A.Mason, "Optical phonon interaction effects in layered semiconductor structures", Annals of Physics **163**, 78 (1985).

[65] M.H.Degani and O.Hipólito, "Electron-polar optical phonon-scattering rates in multisubband quantum wire structures", Surface Science **229**, 279 (1990).

[66] S.Briggs and J.P.Leburton, "Size effects in multisubband quantum wire structures", Physical Review B **38**, 8163 (1988).

[67] J.C.Ryan and T.L.Reinecke, "Band-gap renormalization of optically excited semiconductor quantum wells", Physical Review B **47**, 9615 (1993).

[68] G.Fasol, M.Tanaka, H.Sakaki, and Y.Horikoshi, "Interface roughness and the dispersion of confined LO-phonons in GaAs / AlAs quantum wells", Physical Review B **38**, 6056 (1988).

[69] M.A.Stroscio, "Interaction between longitudinal-optical-phonon modes of a rectangular quantum wire and charge carriers of one-dimensional electron gas", Physical Review B **40**, 6428 (1989).

[70] H.Rücker, E.Molinari, P.Lugli, "Microscopic calculation of the electron-phonon interaction in quantum wells", Physical Review B **45**, 6747 (1992).

[71] J.K.Jain, S.Das Sarma, "Role of discrete slab phonons in carrier relaxation in semiconductor quantum wells", Physical Review Letters **62**, 2305 (1989); K.Mori, T.Ando, "Electron-optical phonon interaction in single and double heterostructures", Physical Review B **40**, 6175 (1989); *ibid.* S.Rudin, T.L.Reinecke, "Electron–LO-phonon scattering rates in multisubband quantum wire structures", **41**, 7713 (1990).

[72] B. K. Ridley, "Electron-scattering by confined LO-polar phonons in a quantum well", Physical Review B **39**, 5282 (1989); B. K. Ridley, M. Babiker, "Continuum-theories of optical phonons and polaritons in superlattices - A brief critique", Physical Review B **43**, 9096 (1991).

[73] I.S.Gradshteyn and I.M.Ryzhik, *Tables of Integrals, Series, and Products* (Academic, New York, 1980).

[74] M.Abramowitz and I.A.Stegun, *Handbook of Mathematical Functions*, (Dover, New York, 1965).